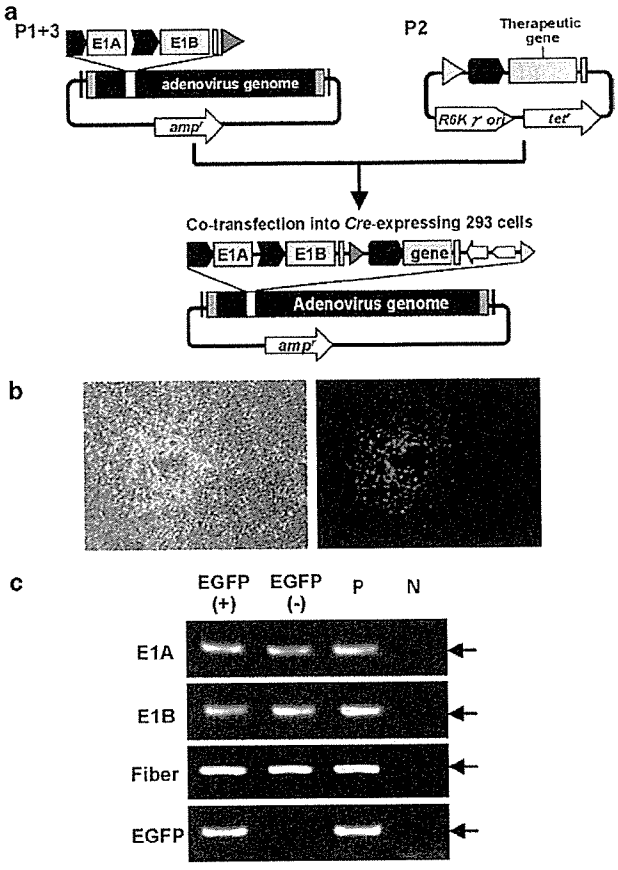

Figure 4 Therapeutic gene insertion into m-CRA directly in Cre-expressing 293 cells (alternative protocol). (a) The schematic representation. (b) Phase-contrast (left) and fluorescent (right) microscopic pictures of an m-CRA plaque (CRA.CEApr-E1A-CMVpr-E1BΔ55kD/CMVpr-EGFP) on Cre-expressing 293 cells 12 days after co-transfection of P1+3 (pAd.HM4-CEApr-E1A-CMVpr-E1BΔ55kD) and P2 (pUni/CMVpr-EGFP). (c) PCR analyses of genomic DNA extracted from m-CRA plaques that do or do not show EGFP fluorescence (two left lanes, respectively). PCR analyses were performed using four different primer sets of S-E1A-1/AS-E1A-1, S-E1B-1/AS-E1B-1, S-Fiber/AS-Fiber, and S-EGFP/AS-EGFP to detect E1A, E1B, fiber, and EGFP DNA, respectively. P, positive control plasmid DNA corresponding to each of primer sets. N, nontemplate DNA.

P2 (pUni/CMVpr-EGFP) were cotransfected into *Cre*-expressing 293 cells. Some plaques became visible 6 days afterwards, and 10 plaques per 10 cm dish appeared 12 days after cotransfection. One of these 10 plaques showed an EGFP-positive finding under fluorescent microscopy (Figure 4b). PCR analysis of the DNA isolated from these plaques verified that only this fluorescence-positive plaque contained a correctly recombined m-CRA with EGFP cDNA (Figure 4c). Therefore, using a marker gene such as *EGFP*, the correct m-CRA derived from P1+2+3 plasmid can be easily isolated from the m-CRA derived from P1+3 plasmid.

Discussion

The large size of the adenoviral DNA (36 kB) hampered the feasible modification of the Ad vector, due to limited numbers of available unique restriction enzyme recognition sites. For constructing the E1-deleted Ad, a two-plasmid system, that is, separate construction of the therapeutic gene and adenoviral backbone in two plasmids, was recently utilized.[23] However, when constructing CRAs, a modification of the E1 region is additionally necessary; currently, there is no standardized method to construct diverse types of m-CRAs in large numbers. Owing to this deficiency, many molecular biologists or gene therapy researchers, who are not CRA specialists, may not be able to efficiently construct CRAs, whereas they can feasibly construct E1-deleted Ad using commercially available kits. Detailed protocols, incorporating the careful consideration of available restriction enzyme sites, should be formulated each time a new CRA is constructed or any time a currently available CRA is modified. The procedures used currently may vary in the details of constructing different m-CRAs, and additional modifications of their own protocols in individual laboratories may be necessary depending on individual CRAs. Thus, even though it may be possible to construct an m-CRA, the present methods are not yet standardized and are deficient in their potential to be widely utilized by a large number of researchers.

In this respect, the notable feature of our system is that it allows the independent and unrestricted construction of individual elements of viral replication, therapeutic genes, and adenoviral backbones in three plasmids, and subsequently permits the accurate fusion of these plasmids within the same protocol into a single m-CRA plasmid without regular ligation procedures. This feature enables a normally trained molecular biologist to feasibly construct m-CRAs, and to construct and/or modify diverse m-CRAs in large numbers. To this end, we introduced *Cre/lox* recombination and I-*Ceu*I/PI-*Sce*I-based ligation for combining the three plasmids, and different types of antibiotic resistance genes and *ori* for specifically selecting only the correctly combined clones, into this system. In this context, the factors needed for this system to function at its maximum efficiency were the use of both an optimized concentration of tetracycline, and high-activity *Cre*. Due to the fact that there have been no reports of tetracycline selection together with the *Cre/lox* recombination in *E. coli*, and because we obtained a lower transformation efficiency with tetracycline than with kanamycin or ampicilin, we initially determined the optimal concentration of tetracycline for this system. Unexpectedly, the optimal concentration of tetracycline was 5 μg/ml in the LB plate, which is lower than that described in textbooks (12 μg/ml),[27] and the effective range was narrow (data not shown). Higher *Cre* activity is also essential, especially due to the use of tetracycline selection; the use of lower *Cre* activity did not result in the appearance of the correct clone. We established a feasible and inexpensive way to obtain aliquots containing highly active *Cre*. With these conditions, sufficient numbers of clones always appeared, and all of them contained the correct recombined plasmid. The distinct advantage of the present method is 100% accuracy of correct clones among all of the transformed clones in *E. coli*; this feature, together with the use of miniprep DNA throughout the procedure, allowed us to handle multiple diverse samples at one time, and we in fact simultaneously constructed diverse types of m-CRAs in this study. The remnant components of *tet*^{r}, *R6Kγ ori*, and a single *lox* sequence in m-CRAs, which are indispensable to achieve 100% accuracy of correct clones,

are not troublesome, at least for the experimental purpose, probably in general, described herein because neither *tet*^{r} lacking a proper mammalian promoter or poly A sequence, nor *R6Kγ ori* efficiently function in mammalian cells. In fact, we found that several m-CRAs, including the ones shown in Figure 3c in this study, function well with these components without any harmful effects.

An introduction of a marker gene into a CRA, such as *EGFP* gene used in the present study, which allows researchers to monitor the spread of a CRA *in vitro* and *in vivo*, is quite useful for carefully analyzing the virological features of CRA. It was recently shown that CRA expressing a therapeutic gene may enhance the cytotoxicity and the therapeutic potential in addition to the oncolytic activity of CRAs.[19] In this regard, an advantage of our system is the ability to subsequently insert a therapeutic or marker gene either into an m-CRA plasmid in *E. coli* or directly into m-CRA in *Cre*-expressing 293 cells. To maximize both protocols, diverse types of P1+3 and P2 may be initially prepared using the regular subcloning procedure, because combining different types of P1+3 and P2 at the later stage can be carried out simultaneously, as shown in the present study. The latter protocol, that is, direct transfection of P1+3 and P2 into *Cre*-expressing 293 cells, has the advantage of further eliminating one step in *E. coli*, leading to an increase in the rapidity of the procedure. *EGFP* or other fluorescent genes alongside the therapeutic gene in P2, which allows direct identification of the correct m-CRA plaque containing therapeutic genes under fluorescent microscopy, may maximize this benefit.

The unrestricted and independent construction of individual elements in the three-plasmid system should not only expedite the process of generating diverse m-CRAs but also make feasible the modification of individual elements in m-CRAs. Several combination patterns of different P1, P2, and P3 vectors allow the generation of diverse types of m-CRAs in large numbers, including those in which some elements were modified with diverse combinations. Lessons from previous gene therapy studies, that is, discrepancies between experimental data and actual clinical outcomes, suggest the necessity of the systematic and extensive examination of the biological and virological characteristics of diverse m-CRAs in practice. In this respect, the ability to efficiently generate large numbers of modified m-CRAs with diverse combinations of gene elements may be the most significant advantage of our system. Particularly, unrestricted selection of the adenoviral backbone may provide two potential advantages. First, any suitable adenoviral backbone, such as fiber-modified Ads to achieve tumor-specific infection, which may be determined by other types of extensive studies, can be directly used in the m-CRA studies; additional steps in constructing new m-CRAs that contain both characteristic elements may be omitted. Second, Ad can package 105% of its genome, and such DNA size limitation may potentially complicate or hamper the modification of pre-constructed m-CRAs. However, the present system allows the change of the P3 backbone plasmid to circumvent this problem; P3 with a longer deletion can be used if additional DNA should be inserted in P1 or P2 to modify pre-established m-CRA. Namely, the three-plasmid system in the present m-CRA construction may maximize the benefit of the *in vitro* ligation system.[23] For instance, up to 5.4, 5.9 or 8.7 kb of DNA elements can be introduced in P1 and P2 when pAdHM4, pAdHM10, or pAdHM12 is used as P3 vector, respectively, as described previously.[23]

In conclusion, the present study reports a novel method for efficiently constructing and/or modifying diverse m-CRAs; this system may be useful for the development of the ideal m-CRA for tumor therapy.

Materials and methods

Cell lines

The human hepatoma cell line, Hep-G2, was obtained from the Cell Resource Center for Biomedical Research at the Institute of Development, Aging and Cancer, Tohoku University (Sendai, Japan). Hep-G2 was cultured in Dulbecco's modified Eagle's medium supplemented with 100 U/ml penicillin, 100 μg/ml streptomycin, and 10% fetal bovine serum. The *Cre*-expressing 293 cell line was generated as described elsewhere.[28]

Plasmids

Plasmid P1 was constructed as follows. The E1A coding sequence and pA without the native E1A promoter were obtained by PCR from pXC1 (Microbix, Toronto, Canada) with the primers S-E1A/AS-E1A (Table 1). This E1A fragment was digested with *Sph*I and *Sal*I and inserted into *Sph*I/*Sal*I-digested pHM5.[23] The resulting plasmid was designated pΔPrE1A. The mt E1B coding sequence (1684–2285), which lacked the E1B55kD coding sequence, native E1B promoter, and pA, was obtained by PCR from pXC1 with the primers S-E1BΔ55kD/AS-E1BΔ55kD (Table 1) and inserted into pΔPrE1A by *Sal*I/*Bam*HI sites, resulting in pΔPrE1A-ΔPrE1BΔ55kDΔpA plasmid. BGHpA obtained by PCR with the primers S-BGHpA/AS-BGHpA (Table 1) from pRc/CMV plasmid (Invitrogen, Carlsbad, CA, USA) was inserted into pΔPrE1A-ΔPrE1BΔ55kDΔpA by *Bam*HI/*Eco*RI sites, resulting in pΔPrE1A-ΔPrE1BΔ55kD plasmid. The full length of E1B (1684–4073) was obtained by PCR from pXC1 with the primers S-E1B/AS-E1B (Table 1) and inserted into *Kpn*I/*Eco*RI-digested pΔPrE1A-ΔPrE1BΔ55kD, resulting in ΔPrE1A-ΔPrE1B plasmid. All sequences obtained by PCR were confirmed using an ABI Prism 310 genetic analyzer (Applied Biosystems, Foster City, CA, USA).

E1A sequence without a 24 bp sequence for pRb binding was obtained by site-directed mutagenesis using sequential PCR steps[27] with the primers AS-E1AΔ24/S-E1AΔ24 (Table 1). The obtained product was inserted into pΔPrE1A-ΔPrE1B or pΔPrE1A-ΔPrE1BΔ55kD plasmid by *Not*I/*Sal*I sites, resulting in pΔPrE1AΔ24-ΔPrE1B or pΔPrE1AΔ24-ΔPrE1BΔ55kD plasmid, respectively.

Plasmid P2 was constructed as follows. *kan*^{r} was removed from pUni/V5-HisC (Invitrogen) by *Bgl*II/*Sma*I digestion. A blunt-end fragment of *tet*^{r} obtained from pBR322 (Invitrogen) was inserted into the vector to yield pUni/V5-HisC-*tet*^{r}. The construction of plasmid P3 was performed as described previously.[23]

CEApr[29] and CMVpr were obtained by PCR from AxCEAprTK (Riken gene bank, Tsukuba, Japan) and pRc/CMV with the primer sets of S-CEApr/AS-CEApr and S-CMVpr/AS-CMVpr, respectively (Table 1). The fragment containing CEApr or CMVpr was excised by

Table 1 PCR primers

Primer	*Sequence*	*Annealing temperature (°C)*
S-E1A	5′-TCAGTCGCATGCGCGGCCGCTACGTAACGCGTTACCCGGTGAGTTCCTCAAGAGGC-3′	57
AS-E1A	5′-GGACGTCCTAGGGTCGACGCCCCATTTAACACGCCATGCAAG-3′	
S-E1BΔ55kD	5′-TCAGTCCCTAGGGTCGACCATATGGATATCCAATTGCGTGGGCTAATCTTGGTTACATCT-3′	57
AS-E1BΔ55kD	5′-GGACGTGGATCCGCGTCTCAGTTCTGGATACAGTTC-3′	
S-E1B	5′ATAAATGGAGCGAAGAAACC -3′	57
AS-E1B	5′-GGACGTGAATTCATAACTTCGTATAATGTATGCTATATGAGGTAATCTTGATCCAAATCCAAACAGAGTC-3′	
S-BGHpA	5′-TCAGTCGGATCCGCATGCATCTAGAGCTCGCTGATC-3′	57
AS-BGHpA	5′-GGACGTGAATTCATAACTTCGTATAATGTATGCTATATGAGGTAATTCAGAAGCCATAGAGCCCACCGCA-3′	
S-Δ24	5′-TTGTACCGGAGGTGATCGATCCACCCAGT-3′	57
AS-Δ24	5′-TCCTCGTCGTCACTGGGTGGATCGATCACC-3′	
S-CEApr	5′-TCAGTCGCGGCCGCATCATCCCACCTTCCCAGAG-3′	57
AS-CEApr	5′-GGACGTACGCGTCCATGGTCTCTGCTGTCTGC-3′	
S-CMVpr	5′-TCAGTCGTCGACCGTTGACATTGATTATTGAC-3′	57
AS-CMVpr	5′-GGACGTCAATTGGCTTGGGTCTCCCTATAGTG-3′	
S-E1A-1	5′-CCTGTGGCATGTTTGTCTAC-3′	57
AS-E1A-1	5′-CAACTGGTTTAATGGGGCAC-3′	
S-E1B-1	5′-AAGGAGGATTACAAGTGGGA-3′	57
AS-E1B-1	5′-AGTAGCAGGCGATTCTTGTG-3′	
S-EGFP	5′-CACAAGTTCAGCGTGTCC-3′	59
AS-EGFP	5′-CTTGATGCCGTTCTTCTG-3′	
S-Fiber	5′-GTTCCTGTCCATCCGCACCCACTATCTTCATGTTG-3′	59
AS-Fiber	5′-AGTGGCAGTAGTTAGAGGGGGTGAGGCAGTGATAG-3′	
S-pHM5	5′-AACGGTCCTAAGGTAGCGAA-3′	59

*Not*I/*Mlu*I or *Sal*I/*Mfe*I, respectively, and ligated into similarly digested pΔPrE1A-ΔPrE1BΔ55kD or pΔPrE1AΔ24-ΔPrE1BΔ55kD, resulting in pCEApr-E1A-CMVpr-E1BΔ55kD or pCEApr-E1AΔ24-CMVpr-E1BΔ55kD. Human osteocalcin promoter (OCpr, −834 to +34)[30] and Surv.pr (−173 to −19)[31] were obtained by PCR from genomic DNA (details should be described elsewhere). E2Fpr (−218 to +51)[32] and TERTpr (−181 to +78)[33] were kindly provided by H Fine (National Cancer Institute, Bethesda, MD, USA) and S Kyo (Kanazawa University, Kanazawa, Japan), respectively. P1 plasmids pCEApr-E1A-E2Fpr-E1BΔ55kD, pCEApr-E1AΔ24-E2Fpr-E1BΔ55kD, pE2Fpr-E1A-CMVpr-E1BΔ55kD, pE2Fpr-E1AΔ24-CMVpr-E1BΔ55kD, pOCpr-E1A-CMVpr-E1BΔ55kD, pOCpr-E1AΔ24-CMVpr-E1BΔ55kD, pTERTpr-E1A-CMVpr-E1BΔ55kD, pTERTpr-E1AΔ24-CMVpr-E1BΔ55kD, pTERTpr-E1A-E2Fpr-E1BΔ55kD, and pTERTpr-E1AΔ24-E2Fpr-E1BΔ55kD were constructed in the same manner as described above. pUni/V5-HisC-*tet*^{r} was digested with *Xho*I and blunted, and the blunt-end fragment of CMVpr, which was excised from pCEApr-E1A-CMVpr-E1BΔ55kD, was inserted to yield pUni/CMVpr. The EGFP coding sequence from pEGFP-C1 (Clontech, Palo Alto, CA, USA) was inserted into pUni/CMVpr to obtain pUni/CMVpr-EGFP. In the same manner, Surv.pr was inserted into pUni/V5-HisC-*tet*^{r}, resulting in pUni/Surv.pr. pUni/CMVpr-p53, pUni/CMVpr-tk, pUni/Surv.pr-p53, and pUni/Surv.pr-tk were constructed by insertion of p53 and HSV-tk fragment excised from pCMV-p53 (Clontech) and pAd.RSV-tk (kindly provided by Z Sheng Guo, University of Pittsburgh Cancer Institute, Pittsburgh, PA, USA) into pUni/CMVpr or pUni/Surv.pr.

PCR

The primer sets used in this study are listed in Table 1. The PCR conditions that were used for the m-CRA construction are described earlier. For verification of the correct m-CRAs, PCR of genomic DNA, which was extracted from viral plaques with proteinase K digestion phenol/chloroform purification and ethanol precipitation, was performed with primer sets, as shown in Table 1. The amplified DNA was analyzed by electrophoresis on 1% agarose gel.

Preparation of Ads

All Ads were generated and amplified in 293 cells, and purified in CsCl gradients, as described previously.[5,23] The titer of the Ads (plaque-forming unit/ml) was measured by a plaque assay on 293 cells.

Acknowledgements

This study was supported in part by a grant for Cooperation of Innovative Technology and Advanced Research in Evolutional Area (CITY AREA) and a Grant-in-Aid for Scientific Research on Priority Areas (C) from the Ministry of Education, Culture, Sports, Science and Technology, Japan, a grant from the Uehara Memorial Foundation and Health and Labour Sciences Research Grants for Third Term Comprehensive Control Research for Cancer from the Ministry of Health, Labour and Welfare, Japan. We thank Izumu Saito, Jun-ichi Miyazaki, Howard Fine, Satoru Kyo, Z Sheng Guo, and Mark A Kay for providing materials and David Cochran for editing the manuscript.

References

1 Terazaki Y *et al*. An optimal therapeutic expression level is crucial for suicide gene therapy for hepatic metastatic cancer in mice. *Hepatology* 2003; 37: 155–163.

2 Fukunaga M *et al.* Adenoviral herpes simplex virus thymidine kinase gene therapy in an orthotopic lung cancer model. *Ann Thorac Surg* 2002; **73**: 1740–1746.
3 Caruso M *et al.* Adenovirus-mediated interleukin-12 gene therapy for metastatic colon carcinoma. *Proc Natl Acad Sci USA* 1996; **93**: 11302–11306.
4 Nagano S *et al.* Gene therapy eradicating distant disseminated micro-metastases by optimal cytokine expression in the primary lesion only: novel concepts for successful cytokine gene therapy. *Int J Oncol* 2004; **24**: 549–558.
5 Chen SH *et al.* Combination gene therapy for liver metastasis of colon carcinoma *in vivo*. *Proc Natl Acad Sci USA* 1995; **92**: 2577–2581.
6 Kruyt FA, Curiel DT. Toward a new generation of conditionally replicating adenoviruses: pairing tumor selectivity with maximal oncolysis. *Hum Gene Ther* 2002; **13**: 485–495.
7 Hallden G, Thorne SH, Yang J, Kirn DH. Replication-selective oncolytic adenoviruses. *Methods Mol Med* 2004; **90**: 71–90.
8 Curiel DT. The development of conditionally replicative adenoviruses for cancer therapy. *Clin Cancer Res* 2000; **6**: 3395–3399.
9 Rodriguez R *et al.* Prostate attenuated replication competent adenovirus (ARCA) CN706: a selective cytotoxic for prostate-specific antigen-positive prostate cancer cells. *Cancer Res* 1997; **57**: 2559–2563.
10 Hallenbeck PL *et al.* A novel tumor-specific replication-restricted adenoviral vector for gene therapy of hepatocellular carcinoma. *Hum Gene Ther* 1999; **10**: 1721–1733.
11 Adachi Y *et al.* A midkine promoter-based conditionally replicative adenovirus for treatment of pediatric solid tumors and bone marrow tumor purging. *Cancer Res* 2001; **61**: 7882–7888.
12 Nettelbeck DM *et al.* Novel oncolytic adenoviruses targeted to melanoma: specific viral replication and cytolysis by expression of E1A mutants from the tyrosinase enhancer/promoter. *Cancer Res* 2002; **62**: 4663–4670.
13 Bischoff JR *et al.* An adenovirus mutant that replicates selectively in p53-deficient human tumor cells. *Science* 1996; **274**: 373–376.
14 Fueyo J *et al.* A mutant oncolytic adenovirus targeting the Rb pathway produces anti-glioma effect *in vivo*. *Oncogene* 2000; **19**: 2–12.
15 Heise C *et al.* An adenovirus E1A mutant that demonstrates potent and selective systemic anti-tumoral efficacy. *Nat Med* 2000; **6**: 1134–1139.
16 Shenk T. Adenoviridae: the viruses and their replication. In: Fields BN, Knipe DM, Howly PM (ed). *Fields Virology.* Lippincott-Raven: Philadelphia, 1996, pp 2111–2147.
17 Harada JN, Berk AJ. p53-Independent and -dependent requirements for E1B-55 K in adenovirus type 5 replication. *J Virol* 1999; **73**: 5333–5344.
18 Rothmann T *et al.* Replication of ONYX-015, a potential anticancer adenovirus, is independent of p53 status in tumor cells. *J Virol* 1998; **72**: 9470–9478.
19 Geoerger B *et al.* Oncolytic activity of p53-expressing conditionally replicative adenovirus Ad{Delta}24-p53 against human malignant glioma. *Cancer Res* 2004; **64**: 5753–5759.
20 Gomez-Manzano C *et al.* A novel E1A-E1B mutant adenovirus induces glioma regression *in vivo*. *Oncogene* 2004; **23**: 1821–1828.
21 Yu DC, Sakamoto GT, Henderson DR. Identification of the transcriptional regulatory sequences of human kallikrein 2 and their use in the construction of calydon virus 764, an attenuated replication competent adenovirus for prostate cancer therapy. *Cancer Res* 1999; **59**: 1498–1504.
22 Johnson L *et al.* Selectively replicating adenoviruses targeting deregulated E2F activity are potent, systemic antitumor agents. *Cancer Cell* 2002; **1**: 325–337.
23 Mizuguchi H, Kay MA. Efficient construction of a recombinant adenovirus vector by an improved *in vitro* ligation method. *Hum Gene Ther* 1998; **9**: 2577–2583.
24 Miyake S *et al.* Efficient generation of recombinant adenoviruses using adenovirus DNA-terminal protein complex and a cosmid bearing the full-length virus genome. *Proc Natl Acad Sci USA* 1996; **93**: 1320–1324.
25 Chartier C *et al.* Efficient generation of recombinant adenovirus vectors by homologous recombination in *Escherichia coli*. *J Virol* 1996; **70**: 4805–4810.
26 Metcalf WW, Jiang W, Wanner BL. Use of the rep technique for allele replacement to construct new *Escherichia coli* hosts for maintenance of R6 K gamma origin plasmids at different copy numbers. *Gene* 1994; **138**: 1–7.
27 Ausubel FM (ed). *Current Protocols in Molecular Biology.* John Wiley & Sons: New York, 1999.
28 Chen L, Anton M, Graham FL. Production and characterization of human 293 cell lines expressing the site-specific recombinase Cre. *Somat Cell Mol Genet* 1996; **22**: 477–488.
29 Osaki T *et al.* Gene therapy for carcinoembryonic antigen-producing human lung cancer cells by cell type-specific expression of herpes simplex virus thymidine kinase gene. *Cancer Res* 1994; **54**: 5258–5261.
30 Yeung F *et al.* Regulation of human osteocalcin promoter in hormone-independent human prostate cancer cells. *J Biol Chem* 2002; **277**: 2468–2476.
31 Li F, Altieri DC. The cancer antiapoptosis mouse survivin gene: characterization of locus and transcriptional requirements of basal and cell cycle-dependent expression. *Cancer Res* 1999; **59**: 3143–3151.
32 Parr MJ *et al.* Tumor-selective transgene expression *in vivo* mediated by an E2F-responsive adenoviral vector. *Nat Med* 1997; **3**: 1145–1149.
33 Takakura M *et al.* Cloning of human telomerase catalytic subunit (hTERT) gene promoter and identification of proximal core promoter sequences essential for transcriptional activation in immortalized and cancer cells. *Cancer Res* 1999; **59**: 551–557.

Supplementary Information accompanies the paper on Gene Therapy website (http://www.nature.com/gt)

INTERNATIONAL JOURNAL OF ONCOLOGY 27: 77-85, 2005

Adenoviral gene transduction of hepatocyte growth factor elicits inhibitory effects for hepatoma

KENTARO YUGE[1,3], TOMOYUKI TAKAHASHI[1,4,7], SATOSHI NAGANO[7,8], YASUHIRO TERAZAKI[5], YOSHITERU MUROFUSHI[1,7], HIROAKI USHIKOSHI[1,2], TAKAO KAWAI[1,2], NGIN CIN KHAI[1,2], TOSHIKAZU NAKAMURA[9], HISAYOSHI FUJIWARA[2] and KEN-ICHIRO KOSAI[1,6,7]

[1]Department of Gene Therapy and Regenerative Medicine, Gifu University School of Medicine; [2]Department of Cardiology, Respiratory and Nephrology, Regeneration & Advanced Medical Science, Graduate School of Medicine, Gifu University, 1-1 Yanagido, Gifu 501-1194; [3]First Department of Internal Medicine, [4]Department of Advanced Therapeutics and Regenerative Medicine, Departments of [5]Surgery and [6]Pediatrics and Child Health, Kurume University School of Medicine, and [7]Division of Gene Therapy and Regenerative Medicine, Cognitive and Molecular Research Institute of Brain Diseases, Kurume University, 67 Asahi-machi, Kurume 830-0011; [8]Department of Orthopaedics, Faculty of Medicine, Kagoshima University, 8-35-1 Sakuragaoka, Kagoshima 890-8520; [9]Division of Molecular Regenerative Medicine, Course of Advanced Medicine, Osaka University Graduate School of Medicine, 2-2 Yamadaoka, Suita 565-0871, Japan

Received November 29, 2004; Accepted February 3, 2005

Abstract. Hepatocyte growth factor (HGF) gene therapy may have potential for treating chronic hepatitis (CH) and liver cirrhosis (LC). However, the lack of an HGF gene therapy study on hepatomas that are often associated with CH or LC, together with the stimulatory effects of HGF on many types of cancer, may hamper its application. This study explored the effects of adenoviral HGF gene transduction and their mechanisms on two types of hepatoma cells (hepatoblastoma and hepatocellular carcinoma) in *in vitro* experiments. Both types of hepatomas were revealed to have higher adenoviral gene transduction efficiencies and more efficient expressions of the HGF transgene, which successfully activated the HGF receptor/c-Met in an autocrine fashion, than those of other types of cancer. Notably, not only HGF, but also adenoviral infection, inhibited DNA synthesis, whereas only HGF but not adenoviral infection exerted a potent apoptotic effect. Moreover, adenoviral HGF gene transduction additively exerted inhibitory effects on cisplatin-treated hepatomas. In conclusion, inhibitory and apoptotic effects of adenoviral HGF gene transduction in hepatomas in contrast to potent mitogenic and antiapoptotic effects of HGF for hepatocytes are not only of biological interest, but also pose clinical benefits for adenoviral HGF gene therapy for CH and LC.

Correspondence to: Dr Ken-Ichiro Kosai, Division of Gene Therapy and Regenerative Medicine, Cognitive and Molecular Research Institute of Brain Diseases, Kurume University, 67 Asahi-machi, Kurume 830-0011, Japan
E-mail: kosai@med.kurume-u.ac.jp

Abbreviations: Ad, adenoviral vector; AGTE, adenoviral gene transduction efficiency; MOI, multiplicity of infection; RSV, Rous sarcoma virus long terminal repeat; X-gal, o-nitrophenyl-ß-D-galactophyranoside; ELISA, enzyme-linked immunosorbent assay

Key words: adenoviral vector, hepatocyte growth factor, hepatoma, apoptosis, DNA synthesis, cisplatin

Introduction

Hepatocyte growth factor (HGF), originally identified (1-4) and cloned (5,6) as a potent mitogen for hepatocytes, is a multifunctional cytokine that exhibits mitogenic, motogenic, morphologic, angiogeneic, antiapoptotic and organotrophic effects on a variety of tissues (7). We recently showed that HGF exerts a potent antiapoptotic effect on hepatocytes and antifibrotic effects, and can be used to treat acute hepatitis, including fulminant hepatic failure (8,9), and chronic hepatitis (CH) and liver cirrhosis (LC) in animals (10-12). Thus, these beneficial effects, together with the inducible effect for liver regeneration (13), suggest that HGF gene therapy may be a promising treatment for CH and LC.

However, certain types of growth factors may play important roles in the carcinogenesis, tumor growth, and angiogenesis of cancer. Accumulating data suggest that HGF may enhance the growth and metastases of a majority of cancers, probably due not only to direct stimulation of cancer cell growth, but to the enhancement of angiogenesis (14,15). In fact, the HGF antagonist has been shown to inhibit cancer cell growth, metastasis, and angiogenesis of some cancers in animals (16,17). In contrast, other studies suggested that HGF might exert an inhibitory effect on certain types of cancers (18-23) although their overall features and mechanisms remain obscure.

In particular, the roles and effects of HGF on hepatomas remain largely controversial. In transgenic mouse (Tg) studies,

two distinct types of HGF Tg, in which HGF was overexpressed under the transcriptional control of either the hepatocyte-specific albumin promoter (Alb-HGF-Tg) (24) or the ubiquitously active mouse metallothionein gene promoter (MT-HGF-Tg) (25,26), demonstrated completely opposite results concerning hepatocarcinogenesis. Alb-HGF-Tg never formed a hepatocellular carcinoma (HCC), and furthermore, analyses using two kinds of double Tg; Alb-HGF/MT-TGF-α Tg (27) and Alb-HGF/Alb-*c-myc*-Tg (28), showed that the overexpression of HGF in hepatocytes inhibited both TGF-α and c-myc-induced hepatocarcinogenesis. In contrast, MT-HGF-Tg formed cancers in several organs, including HCC in the liver (25,26). Thus, rather than elucidating this issue, these Tg studies have led to confusion, probably due to the artificial factors in the studies. On the other hand, *in vitro* studies have recently shown that recombinant HGF has an inhibitory effect on the human hepatoblastoma cell line, HepG2 (29), but no study has as yet explored the effects of HGF on human hepatocellular carcinoma (HCC). More importantly, there has not only been no direct studies of HGF gene therapy for hepatoma, but also no biological studies of adenoviral HGF gene transduction in hepatomas, including no investigation of the effects of adenoviral infection itself or the effects of exogenous HGF gene expression in an artificial autocrine fashion.

HCC, which is the major type of hepatoma found in adult patients, is usually associated with CH or LC. Alternatively, CH and LC have a high risk of hepatocarcinogenesis (30-32), and some patients with CH and/or LC may potentially have latent HCC at an undetectably small size. Thus, although HGF gene therapy may have potential for treating CH and LC, its clinical application may be prohibited due to the uncertain effects of HGF gene therapy for hepatomas. In this regard, the present study biologically explored the effect of adenoviral HGF gene transduction in hepatoma cells and its mechanism.

Materials and methods

Human cell lines. The human cell lines Hep3B (HCC), HepG2 (hepatoblastoma), HeLa (cervical carcinoma), MKN-28 (gastric carcinoma), colo-205 (colon carcinoma), HOS-NP (osteosarcoma), A549 (lung carcinoma) and 293, were cultured in 5% CO_2 at 37°C in Dulbecco's modified Eagle's medium supplemented with penicillin/streptomycin and 10% fetal calf serum.

Recombinant adenoviral vectors (Ads) and adenoviral gene transduction efficiencies (AGTEs). Replication-defective Ads, Ad.RSV-HGF and Ad.RSV-LacZ, which encode the human HGF and ß-galactosidase gene, respectively, downstream of the transcriptional control of the Rous sarcoma virus long terminal repeat (RSV) promoter were constructed, prepared, and titered as described previously (33-35). AGTEs were assessed by 5-bromo-4-chloro-3-indolyl-ß-D-galactopyranoside (X-gal) staining after Ad.RSV-LacZ infection, as described previously (36-38).

HGF enzyme-linked immunosorbent assay (ELISA). HeLa, Hep3B and HepG2 cells at 1000, 1000 and 2000 cells/well in 96-well plates, respectively, were infected with Ad.RSV-HGF, and the supernatant was collected 48 or 96 h later. The human HGF levels in the supernatant were measured by ELISA according to the manufacturer's protocol (R&D Systems, Inc., Minneapolis, MN).

C-Met phosphorylation. C-Met phosphorylation in the cells was detected by the immunoprecipitation method (39). Briefly, the cells were lysed in 500 µl RIPA buffer (1% Triton X, 150 mM NaCl, 50 mM Tris-HCl pH 7.6, 10% glycerol, 1 mM Vanadate, 1 mM phenylmethylsulfonyl fluoride) with protease inhibitors after incubation with the serum-free media for 24 h and subsequently with new serum-free media containing recombinant HGF (R&D Systems) or the supernatant from Ad.RSV-HGF-infected HepG2 cells for 10 min. After centrifugation, the supernatant was incubated with 0.5 ng/ml anti-c-Met monoclonal antibody (C-12, Santa Cruz Biotechnology, Inc., Santa Cruz, CA) for 4 h, and sequentially incubated with 10 µl Protein G Sepharose beads for 3 h. The proteins bound to beads were dissolved in sample buffer and subjected to sodium dodecyl sulfate-polyacrylamide gel electrophoresis (SDS-PAGE). Phosphorylated c-Met was immunoblotted with anti-phosphotyrosine antibody (PY20, Transduction Laboratories, Lexington, KY).

WST-8 cell viability assay. The cells were infected with each Ad in the same manner as in the HGF ELISA experiment. Cell viability was determined by WST-8 assay (Dojindo Laboratories Co., Mashiki, Japan) at 2, 4, 6 or 8 days after Ad infection according to the manufacturer's protocol (36,37).

To explore the effect of HGF in cisplatin (cis-Diammine-dichloroplatinum (II))-treated hepatoma cells, cisplatin was added to the media in the HepG2 and HeLa cells (125 µg/ml) and in the Hep3B cells (250 µg/ml) at 24 h after Ad-infection.

Bromo-2'-deoxyuridine (BrdU) uptake assay. The cells were infected with each Ad in the same manner as in the HGF ELISA experiments. Four days later, the cells were incubated with 10 µM of BrdU for 4 h and harvested. The percentage of cells that had BrdU uptake was measured by ELISA according to the manufacturer's protocol (BrdU Labeling and Detection Kit III, Roche Diagnostics GmbH, Mannheim, Germany).

Terminal deoxynucleotidyl transferase-mediated deoxyuridine triphosphate biotin nick-end labelling (TUNEL) assay. Hep3B or HeLa ($1x10^5$) cells, or HepG2 ($2x10^5$) cells were infected with each Ad, and apoptotic cells were detected at 2, 4, 6 or 8 days later using an ApopTag Peroxidase *in situ* Apoptosis Detection Kit (Intergen Company, New York, USA) according to the manufacturer's protocols.

Detection of active form of caspase-3. The cells were lysed in hypotonic buffer (25 mM HEPES pH 7.5, 5 mmol/l $MgCl_2$, 1 mmol/l EDTA, 1 mmol/l phenylmethylsulfonyl fluoride) with protease inhibitors at 2, 3 or 4 days after adenoviral infection at the multiplicity of infection (MOI) of 10. Protein (30 µg) was subjected to SDS-PAGE, and Western blotting was performed using anti-caspase-3 antibody (BD Pharmingen, San Diego, CA), peroxidase-conjugated anti-rabbit IgG and

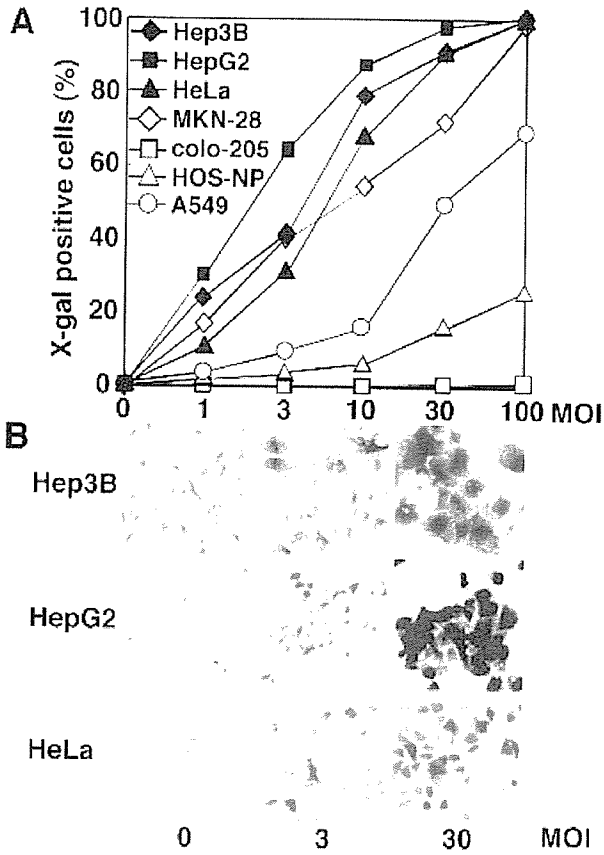

Figure 1. AGTEs. Cells were infected with Ad.RSV-LacZ at indicated MOIs and stained with X-gal. (A), The AGTEs in Hep3B and HepG2 were as high as those in HeLa cells, and higher than those in other types of cells. (B), The representative pictures of X-gal-stained cells.

SuperSignal® West Pico Chemiluminescent Substrate (Pierce Chemical Co., Rockford, IL).

Statistical analysis. All results are expressed as mean ± standard deviation. Statistical comparison were made using Student's t-test.

Results

High AGTE and HGF expression in hepatoma cells. The AGTEs in the Hep3B and HepG2 cells were as high as those in the HeLa cells, and higher than those in other types of human carcinoma cell lines at each MOI (Fig. 1). Because of this, the HeLa cells were chosen as a control for subsequent experiments.

The exogenous human HGF levels in the supernatant were much higher at 48 h than at 96 h after the Ad.RSV-HGF infection in the Hep3B, HepG2 and HeLa cells (Table I). The HGF levels largely differed among these 3 cell lines, and the levels in the HepG2 and Hep3B cells were remarkably higher than those in the HeLa cells at each point. In addition, the HGF levels in the supernatant from the Ad.RSV-HGF-infected MKN-28 cells were much lower than those of the HeLa cells (data not shown). Thus, hepatoma may be a good target for adenoviral HGF gene therapy in terms of the efficient secretion of exogenous HGF in the autocrine mode as well as a high AGTE.

Table I. HGF levels after adenoviral HGF gene transduction.

		HGF levels (ng/ml)	
Cell lines	MOIs	48 h	96 h
Hep3B	0	0.0	0.0
	3	<0.1	0.1
	10	0.1	6.0
	30	1.1	21.7
HepG2	0	0.0	0.0
	3	<0.1	2.1
	10	0.4	83.4
	30	5.9	>4125.0
HeLa	0	0.0	0.0
	3	<0.1	<0.1
	10	<0.1	0.1
	30	0.1	2.7

The supernatant was collected 48 or 96 h after infection with Ad.RSV-HGF at indicated MOIs. The human HGF levels in the supernatant was measured by ELISA.

Exogenous HGF in the autocrine fashion activates HGF receptor/c-Met. Immunoprecipitation and Western blot analysis showed that the Hep3B, HepG2, and HeLa cells were all abundant in the c-Met, which was similarly phosphorylated (i.e., activated) in an HGF dose-dependent manner (Fig. 2A).

HGF natively acts on target cells in a paracrine fashion in the body. Namely, a single chain prepro HGF is secreted from mesenchymal cells and then converted by a specific protease to biologically active mature HGF, which binds to c-Met and confers a biological function in hepatocytes (7). To explore whether transduced HGF in hepatoma cells may function in an artificial autocrine fashion, we initially tried to directly detect c-Met phosphorylation in the Ad.RSV-HGF-infected HepG2 and Hep3B cells. However, several attempts did not result in successful detection because it was difficult to detect short term c-Met phosphorylation under biologically complex circumstances in which persistent HGF expression might lead to repeated cycles of activation, downregulation and the revival of c-Met. Therefore, we indirectly explored the above issue as follows. The supernatant was collected from Ad.RSV-HGF-infected HepG2 cells, and the HGF concentration in it was measured. Subsequently, supernatant or recombinant HGF at the same concentration was added to intact HepG2 (Fig. 2B) or Hep3B cells (data not shown), and the c-Met phosphorylation was explored. As a result, c-Met activation was found to occur in both types of hepatomas in a dose-dependent manner similar to the cases of additions of recombinant HGF, indicating that exogenous HGF protein from the transgene might be efficiently converted to the active form by proteases natively present in the serum, and finally verifying that exogenous HGF correctly activated c-Met.

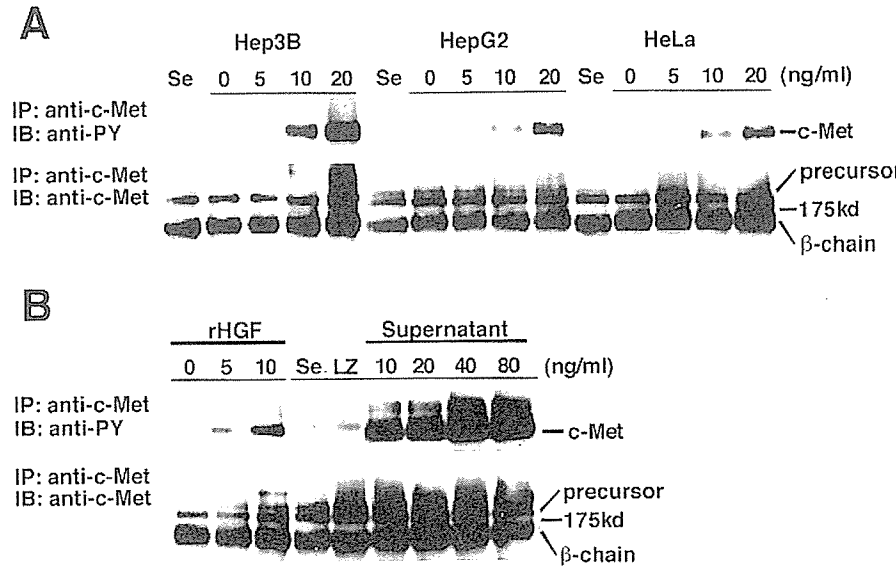

Figure 2. HGF receptor/c-Met and its activation. (A), Hep3B, HepG2 and HeLa cells were abundant in the c-Met, which was similarly phosphorylated in a HGF dose-dependent manner. (B), The c-Met on intact HepG2 cells was similarly phosphorylated by additions of the supernatant from Ad.RSV-HGF-infected HepG2 cells. IP, immunoprecipitation. IB, immunoblot. rHGF, recombinant HGF.

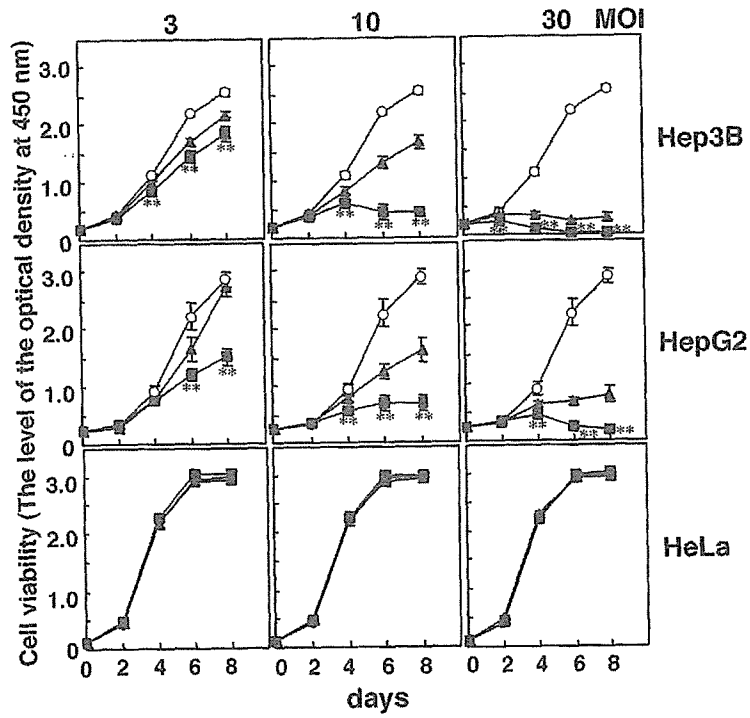

Figure 3. Inhibitory effects of adenoviral HGF gene transduction. Cell viability was determined by WST-8 assay 2, 4, 6 or 8 days after infection with each Ad at indicated MOIs. Although Ad.RSV-LacZ infection as well as Ad.RSV-HGF infection revealed some inhibitory effects for the HepG2 and Hep3B cells, but not for the HeLa cells, the degree of this inhibitory effect was more prominent in the Ad.RSV-HGF-infected cells (square) than the Ad.RSV-LacZ-infected ones (triangle). *P<0.05; **P<0.01 (Ad.RSV-HGF versus Ad.RSV-LacZ groups on each day at each MOI). No treatment control, circle. N=8, each point in each group.

Ad.RSV-HGF infection exerts inhibitory effects for hepatoma cells. The WST-8 assay showed that the number of viable Hep3B and HepG2 cells was significantly smaller in the Ad.RSV-HGF-infected cells than in the Ad.RSV-LacZ-infected cells at each MOI (Fig. 3). In addition, the infection of Ad.RSV-LacZ revealed some inhibitory effects for the HepG2 and Hep3B cells in an Ad dose-dependent manner, but not for the control HeLa cells, although the degree of this inhibitory effect was milder than that by Ad.RSV-HGF. In contrast, there was no difference in the number of viable HeLa cells among the Ad.RSV-HGF-infected, Ad.RSV-LacZ-infected cells, or no Ad-infected cells at any points. Thus,

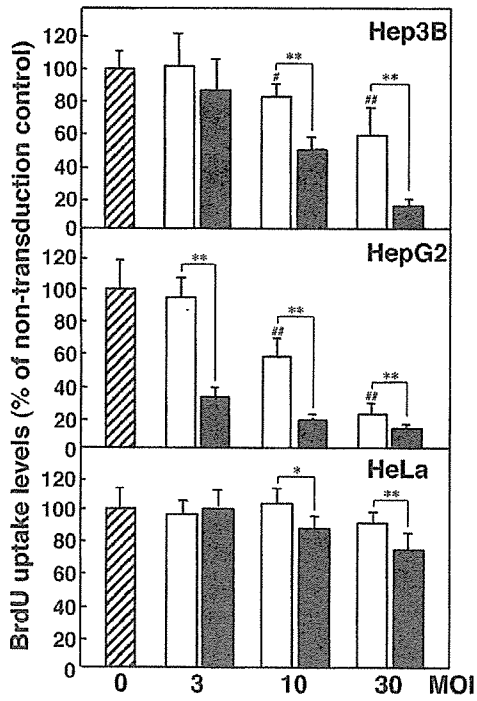

Figure 4. Inhibition of DNA synthesis. BrdU uptake assay was done 4 days after each Ad infection at indicated MOIs. Although the BrdU uptake levels were reduced by Ad.RSV-LacZ infection as well as Ad.RSV-HGF infection in HepG2 and Hep3B cells, the degree of this reduction was more prominent in the Ad.RSV-HGF-infected cells than the Ad.RSV-LacZ-infected ones. The BrdU uptake levels in HeLa cells were mildly reduced by Ad.RSV-HGF infection. $^{*}P<0.05$; $^{**}P<0.01$ (Ad.RSV-HGF groups versus Ad.RSV-LacZ groups at each MOI). $^{\#}P<0.05$; $^{\#\#}P<0.01$ (Ad.RSV-LacZ versus non-transduced control). N=8, each point in each group.

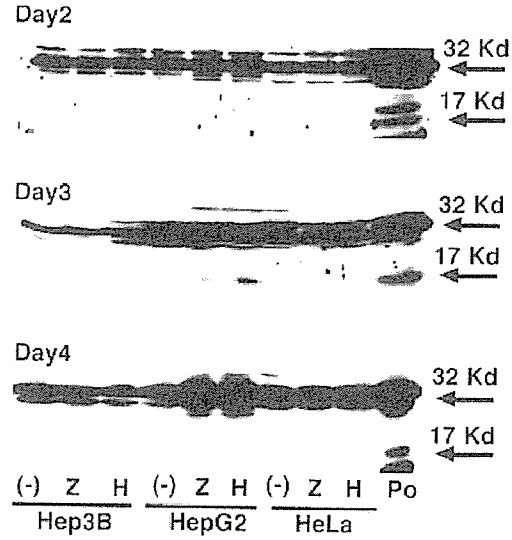

Figure 5. Caspase-3 activation. Pro-caspase-3 (32 kDa) and active caspase-3 (17 kDa) were detected by Western blotting of cells 2, 3, 4 days after no Ad (-), Ad.RSV-LacZ (Z) or Ad.RSV-HGF (H) infection at MOI of 10. Positive control (Po); cisplatin-treated HepG2 cells. More prominent activation of caspase-3 was seen in HepG2 cells 3 days after Ad.RSV-HGF infection than after Ad.RSV-LacZ or no Ad infection.

both types of hepatomas were remarkably sensitive not only to HGF, but also to the adenoviral infection itself, both of which independently and additively exerted inhibitory effects.

Ad.RSV-HGF infection inhibits DNA syntheses of hepatoma cells. There are two possible causes of inhibitory effects; one is the inhibition of cell growth, and the other is the induction of cell death. To assess the former, DNA replication was analyzed by the BrdU uptake assay (Fig. 4). The BrdU uptake levels in the Hep3B and HepG2 cells were both significantly reduced by not only Ad.RSV-HGF, but also by Ad.RSV-LacZ infection in an Ad dose-dependent manner. Statistical differences between the Ad.RSV-HGF and Ad.RSV-LacZ groups at each MOI further indicated that HGF itself inhibited cell growth in both types of hepatomas. The BrdU uptake levels in the HeLa cells were reduced only by Ad.RSV-HGF infection at a high MOI, but not by the adenovirus infection itself. Thus, not only HGF, but also the adenoviral infection itself, independently and additively inhibits cell growth in both types of hepatomas.

HGF but not adenoviral infection exerts apoptotic effect for hepatoma cells. To investigate the apoptotic effect of HGF on hepatomas, the activation of caspase-3, which leads to the activation of important apoptosis-related proteins such as caspase-activated DNase (40) and Acinus (41), was investigated by Western blotting (Fig. 5). Ad.RSV-HGF infection in the HepG2 cells led to a more prominent appearance of the active form of caspase-3 (17 kDa) than that of Ad.RSV-LacZ or no Ad infection. In contrast, a significant activation of caspase-3 was not detected in the Hep3B or HeLa cells after Ad.RSV-HGF, Ad.RSV-LacZ or no Ad infection, despite several trials. In addition, the activation of caspase-3 was not detected in any samples using the CPP32/Caspase-3 Colorimetric Protease Assay Kit (data not shown). Thus, despite substantial technical difficulty with this experimental system, including the issue of abundant pro-caspase-3 in comparison to a limited amount of active caspase-3, the detection of a more prominent band of active caspase-3 in the Ad.RSV-HGF-infected HepG2 cells suggests that exogenous HGF in the autocrine fashion may activate apoptotic signals in hepatoma cells.

We next performed TUNEL assays, which provided clearer and more definitive results (Fig. 6). TUNEL-positive Hep3B and HepG2 cells were significantly increased after the Ad.RSV-HGF infection, in contrast to no increase after the Ad.RSV-LacZ infection. On the other hand, TUNEL-positive HeLa cells were not seen after the Ad.RSV-HGF or Ad.RSV-LacZ infection. These findings indicate that HGF in an autocrine fashion may directly exert a potent apoptotic effect for both types of hepatomas; however, adenoviral infection itself does not induce apoptosis, in contrast to its inhibitory effect on cell growth.

Ad.RSV-HGF infection additively exerts inhibitory effect for cisplatin-treated hepatoma cells. To explore whether adenoviral HGF gene therapy is potentially applicable to hepatoma patients who undergo conventional carcinostatic treatments, we investigated the effect of Ad.RSV-HGF infection on cisplatin-treated hepatoma cells (Fig. 7). We chose cisplatin because cisplatin is one of the representative

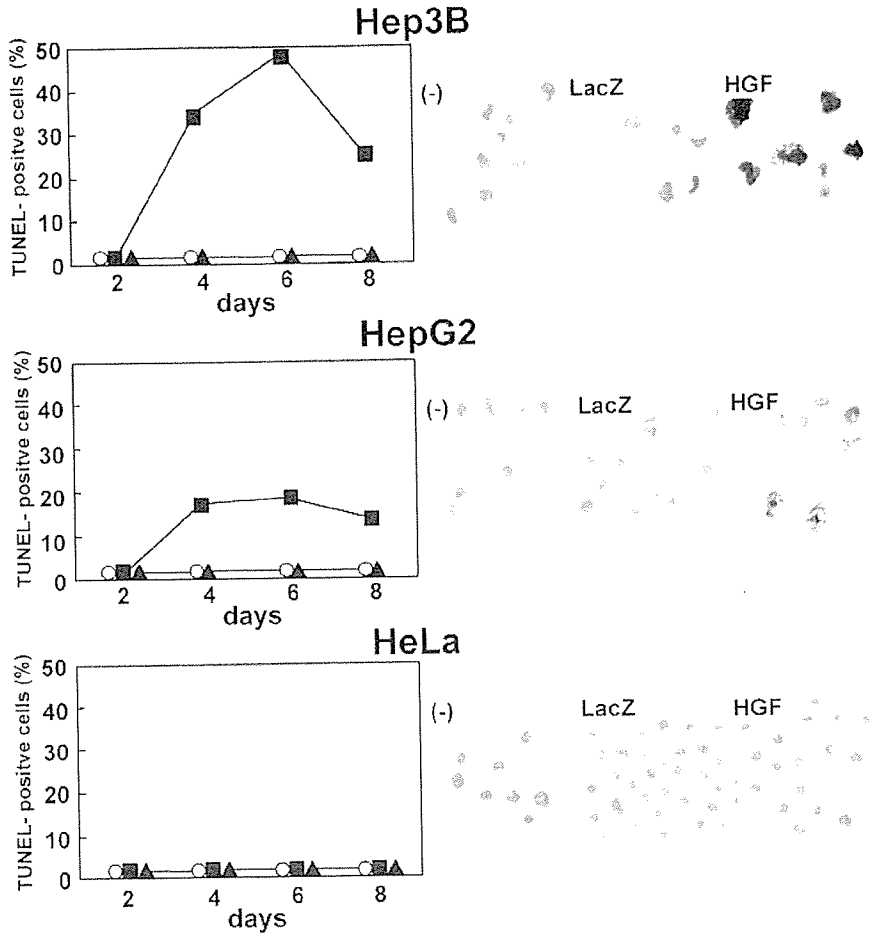

Figure 6. TUNEL assay. TUNEL-positive cells were significantly increased after Ad.RSV-HGF infection in Hep3B and HepG2 cells, but not in HeLa cells. In contrast, TULEL-positive cells were not seen after Ad.RSV-LacZ infection or control (no Ad infection). The circle, triangle and square symbols indicate no Ad-, Ad.RSV-LacZ- or Ad.RSV-HGF-treated groups, respectively. The representative pictures of TUNEL-positive cells 6 days after each Ad infection are shown in the right panel.

carcinostatics for hepatoma patients, especially in the case of transcatheter arterial embolization (TAE) therapy (42,43). WST-8 analysis showed that the Ad.RSV-HGF infection exerted additional inhibitory effects on both Hep3B and HepG2 cells independently and additively to those of cisplatin. Ad.RSV-LacZ infection exerted a milder but apparent inhibitory effect on cisplatin-treated hepatoma cells in an Ad dose-dependent manner. Thus, the effects of HGF, Ad and cisplatin on hepatomas were all inhibitory but independent, and, therefore, the Ad.RSV-HGF infection exerted the most prominent inhibitory effects for hepatoma cells as the result of the additive effects of all 3 factors. In contrast, neither Ad.RSV-HGF nor Ad.RSV-LacZ infection changed the effect of cisplatin in HeLa cells.

Discussion

The present study demonstrated not only that adenoviral HGF gene transduction significantly exhibited inhibitory effects on both HCC and hepatoblastoma, but also that such inhibitory effects were due to both the inhibition of cell growth and the induction of apoptosis.

The opposing activities of HGF, i.e., its antimitotic and mitotic effects and its apoptotic and antiapoptotic effects on hepatoma cells and hepatocytes are of biological interest. In terms of effects on cell growth, the following explanations were suggested by recent studies using HepG2 cells. The sustained duration of p21/waf1 induction might be a determinant of HGF-induced inhibitory effects (44), and integrin-mediated signals from the extracellular matrix could modulate HGF-mediated signals (45). The levels of ERK activity might determine the opposing proliferation responses; HGF-induced growth inhibition was caused by the cell cycle arrest, which resulted from hypophosphorylated pRB via high-intensity ERK signals (29). Although HepG2 cells were solely used for these investigations, some of the findings might be applicable to the different phenotypic effects of HGF between hepatoma cells and hepatocytes; hypothetically, the different responsiveness of these molecules might at least in part determine the differences in HGF-induced signaling between them.

In terms of apoptosis and HGF, a recent study interestingly showed the direct interaction of c-Met and the death receptor Fas in hepatocytes; such interaction prevented Fas self-aggregation and Fas ligand binding, thus inhibiting Fas activation and apoptosis (46). Together with the frequent observation of altered Fas expressions and systems in hepatoma cells (47,48), hypothetically, an altered Fas system in

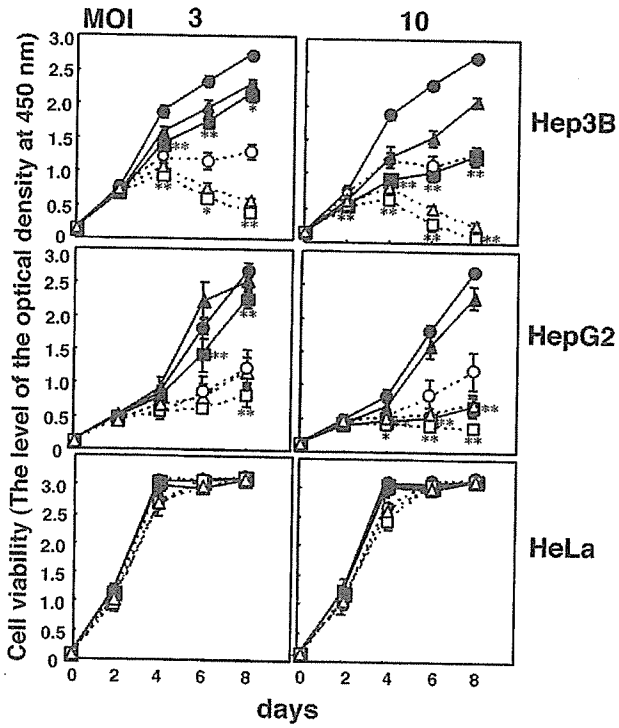

Figure 7. Additive inhibitory effects of Ad.RSV-HGF for cisplatin-treated hepatoma cells. Cell viability after infection with each Ad with or without cisplatin was determined by WST-8 assay. Although Ad.RSV-LacZ infection as well as Ad.RSV-HGF infection revealed additional inhibitory effects for HepG2 and Hep3B cells, but not for HeLa cells, additively to those of cisplatin, the degrees of the inhibitory effects were more prominent in the Ad.RSV-HGF-infected cells than those in the Ad.RSV-LacZ-infected ones. The open or closed symbols are indicated as the groups treated with or without cisplatin, respectively, while the circle, triangle and square symbols indicate no Ad-, Ad.RSV-LacZ- or Ad.RSV-HGF-treated groups, respectively. $^{*}P<0.05$, $^{**}P<0.01$ (Ad.RSV-LacZ groups versus Ad.RSV-HGF groups on each day at each MOI). N=8, each point in each group.

hepatomas might mean that the sequestration of Fas is lost by the c-Met and HGF-induced antiapoptotic effect in hepatomas. Although the identification of the molecules that were involved in these features were not the focus of the present study, overall elucidation in future studies may not only be of biological interest, but clinically useful for developing more effective HGF gene therapy.

On the other hand, the present study revealed clinically important information. The beneficial data obtained here may allow for the clinical application of adenoviral HGF gene therapy for CH and LC. First, high AGTE and the efficient expressions of exogenous HGF in an autocrine fashion in hepatomas may suggest that hepatomas are a good target site for gene transduction in the case of adenoviral HGF gene therapy for associated CH or LC; adenovirus-associated hepatotoxicity may be reduced. Second, the inhibitory effects of adenoviral HGF gene transduction for hepatomas, which resulted from not only the HGF-induced and Ad-induced inhibition of cell growth but also the HGF-induced apoptotic effects, are obviously encouraging for treating hepatoma itself. Another encouraging result was that Ad-induced and HGF-induced inhibitory effects were found to additively enhance (rather than diminish) cisplatin-induced cytotoxicity against hepatoma. Several mechanisms of the cisplatin-induced inhibitory effects have been reported, including cell cycle arrest by activating the CDK kinase inhibitor (49), and the induction of apoptosis by upregulating Fas and the Fas ligand (50,51). On the other hand, previous studies demonstrated that recombinant Ad induced cell cycle dysregulation by causing the inappropriate expression of cyclin proteins and down-regulation of E2F-1 independent of the Rb and p53 status (52,53). The present results suggest that each signal transduction pathway induced by cisplatin, adenovirus or HGF, including the unknown pathway mentioned above, may not directly cross-talk with each other. Thus, the additive and independent inhibitory effects of Ad, HGF and cisplatin against hepatomas may be clinically beneficial because HGF gene therapy may be not only applicable to, but also therapeutic for, hepatoma patients undergoing treatment with cisplatin.

To further verify such clinical implication, we tried to establish clinically-relevant animal models of orthotopic HCC and hepatoblastoma by transplanting Hep3B and HepG2 cells into severe combined immunodeficiency mice, however, high mortality and uncertain tumor formation were obstacles to further therapeutic experiments. On the other hand, the size of subcutaneously implanted tumor was slightly but insignificantly smaller in Ad.HGF-treated mice than that in Ad.LacZ-treated ones in our preliminary experiments (data not shown). However, we did not pursue these results because subcutaneous tumor models have sometimes led to rather misleading results due to the lack of tissue characteristics or native microenvironments (36,37). Likewise, current HCC-Tg models, in which multiple nodules of HCC appear without CH or LC on various schedules, are neither clinically relevant nor useful for assessing the clinical usefulness of gene therapy strategy (25). In this context, the clinically relevant animal model of HCC with LC or CH should be newly generated and the clinical usefulness of HGF gene therapy should be carefully investigated in future studies.

In conclusion, adenoviral HGF gene transduction in human hepatoblastomas and HCC inhibited their growth and induced apoptosis, as well as additively enhancing the cisplatin-induced inhibitory effect. These effects may be beneficial for HGF gene therapy for CH and LC associated with hepatomas.

Acknowledgements

This study was supported by a Grant-in-Aid for Scientific Research (C) from the Japan Society for the Promotion of Science. We thank Nippon Kayaku Co. Ltd. for providing cisplatin.

References

1. Nakamura T, Nawa K and Ichihara A: Partial purification and characterization of hepatocyte growth factor from serum of hepatectomized rats. Biochem Biophys Res Commun 122: 1450-1459, 1984.
2. Russell WE, McGowan JA and Bucher NL: Partial characterization of a hepatocyte growth factor from rat platelets. J Cell Physiol 119: 183-192, 1984.
3. Thaler FJ and Michalopoulos GK: Hepatopoietin A: partial characterization and trypsin activation of a hepatocyte growth factor. Cancer Res 45: 2545-2549, 1985.
4. Gohda E, Tsubouchi H, Nakayama H, Hirono S, Takahashi K, Koura M, Hashimoto S and Daikuhara Y: Human hepatocyte growth factor in plasma from patients with fulminant hepatic failure. Exp Cell Res 166: 139-150, 1986.

5. Nakamura T, Nishizawa T, Hagiya M, Seki T, Shimonishi M, Sugimura A, Tashiro K and Shimizu S: Molecular cloning and expression of human hepatocyte growth factor. Nature 342: 440-443, 1989.
6. Miyazawa K, Tsubouchi H, Naka D, Takahashi K, Okigaki M, Arakaki N, Nakayama H, Hirono S, Sakiyama O, *et al*: Molecular cloning and sequence analysis of cDNA for human hepatocyte growth factor. Biochem Biophys Res Commun 163: 967-973, 1989.
7. Matsumoto K and Nakamura T: Hepatocyte growth factor (HGF) as a tissue organizer for organogenesis and regeneration. Biochem Biophys Res Commun 239: 639-644, 1997.
8. Kosai K, Matsumoto K, Nagata S, Tsujimoto Y and Nakamura T: Abrogation of Fas-induced fulminant hepatic failure in mice by hepatocyte growth factor. Biochem Biophys Res Commun 244: 683-690, 1998.
9. Kosai K, Matsumoto K, Funakoshi H and Nakamura T: Hepatocyte growth factor prevents endotoxin-induced lethal hepatic failure in mice. Hepatology 30: 151-159, 1999.
10. Ueki T, Kaneda Y, Tsutsui H, Nakanishi K, Sawa Y, Morishita R, Matsumoto K, Nakamura T, Takahashi H, Okamoto E and Fujimoto J: Hepatocyte growth factor gene therapy of liver cirrhosis in rats. Nat Med 5: 226-230, 1999.
11. Matsuda Y, Matsumoto K, Ichida T and Nakamura T: Hepatocyte growth factor suppresses the onset of liver cirrhosis and abrogates lethal hepatic dysfunction in rats. J Biochem 118: 643-649, 1995.
12. Matsuda Y, Matsumoto K, Yamada A, Ichida T, Asakura H, Komoriya Y, Nishiyama E and Nakamura T: Preventive and therapeutic effects in rats of hepatocyte growth factor infusion on liver fibrosis/cirrhosis. Hepatology 26: 81-89, 1997.
13. Kosai KI, Finegold MJ, Thi-Huynh BT, Tewson M, Ou CN, Bowles N, Woo SL, Schwall RH and Darlington GJ: Retrovirus-mediated *in vivo* gene transfer in the replicating liver using recombinant hepatocyte growth factor without liver injury or partial hepatectomy. Hum Gene Ther 9: 1293-1301, 1998.
14. Jeffers M, Rong S and Woude GF: Hepatocyte growth factor/scatter factor-Met signaling in tumorigenicity and invasion/metastasis. J Mol Med 74: 505-513, 1996.
15. To CT and Tsao MS: The roles of hepatocyte growth factor/scatter factor and met receptor in human cancers (Review). Oncol Rep 5: 1013-1024, 1998.
16. Date K, Matsumoto K, Kuba K, Shimura H, Tanaka M and Nakamura T: Inhibition of tumor growth and invasion by a four-kringle antagonist (HGF/NK4) for hepatocyte growth factor. Oncogene 17: 3045-3054, 1998.
17. Kuba K, Matsumoto K, Date K, Shimura H, Tanaka M and Nakamura T: HGF/NK4, a four-kringle antagonist of hepatocyte growth factor, is an angiogenesis inhibitor that suppresses tumor growth and metastasis in mice. Cancer Res 60: 6737-6743, 2000.
18. Kan M, Zhang GH, Zarnegar R, Michalopoulos G, Myoken Y, McKeehan WL and Stevens JI: Hepatocyte growth factor/hepatopoietin A stimulates the growth of rat kidney proximal tubule epithelial cells (RPTE), rat nonparenchymal liver cells, human melanoma cells, mouse keratinocytes and stimulates anchorage-independent growth of SV-40 transformed RPTE. Biochem Biophys Res Commun 174: 331-337, 1991.
19. Tajima H, Matsumoto K and Nakamura T: Hepatocyte growth factor has potent anti-proliferative activity in various tumor cell lines. FEBS Lett 291: 229-232, 1991.
20. Shiota G, Rhoads DB, Wang TC, Nakamura T and Schmidt EV: Hepatocyte growth factor inhibits growth of hepatocellular carcinoma cells. Proc Natl Acad Sci USA 89: 373-377, 1992.
21. Miyazaki M, Gohda E, Tsuboi S, Tsubouchi H, Daikuhara Y, Namba M and Yamamoto I: Human hepatocyte growth factor stimulates the growth of HUH-6 clone 5 human hepatoblastoma cells. Cell Biol Int Rep 16: 145-154, 1992.
22. Tajima H, Matsumoto K and Nakamura T: Regulation of cell growth and motility by hepatocyte growth factor and receptor expression in various cell species. Exp Cell Res 202: 423-431, 1992.
23. Liu ML, Mars WM and Michalopoulos GK: Hepatocyte growth factor inhibits cell proliferation *in vivo* of rat hepatocellular carcinomas induced by diethylnitrosamine. Carcinogenesis 16: 841-843, 1995.
24. Shiota G, Wang TC, Nakamura T and Schmidt EV: Hepatocyte growth factor in transgenic mice: effects on hepatocyte growth, liver regeneration and gene expression. Hepatology 19: 962-972, 1994.
25. Sakata H, Takayama H, Sharp R, Rubin JS, Merlino G and La Rochelle WJ: Hepatocyte growth factor/scatter factor overexpression induces growth, abnormal development, and tumor formation in transgenic mouse livers. Cell Growth Differ 7: 1513-1523, 1996.
26. Takayama H, La Rochelle WJ, Sharp R, Otsuka T, Kriebel P, Anver M, Aaronson SA and Merlino G: Diverse tumorigenesis associated with aberrant development in mice overexpressing hepatocyte growth factor/scatter factor. Proc Natl Acad Sci USA 94: 701-706, 1997.
27. Shiota G, Kawasaki H, Nakamura T and Schmidt EV: Characterization of double transgenic mice expressing hepatocyte growth factor and transforming growth factor alpha. Res Commun Mol Pathol Pharmacol 90: 17-24, 1995.
28. Santoni-Rugiu E, Preisegger KH, Kiss A, Audolfsson T, Shiota G, Schmidt EV and Thorgeirsson SS: Inhibition of neoplastic development in the liver by hepatocyte growth factor in a transgenic mouse model. Proc Natl Acad Sci USA 93: 9577-9582, 1996.
29. Tsukada Y, Miyazawa K and Kitamura N: High intensity ERK signal mediates hepatocyte growth factor-induced proliferation inhibition of the human hepatocellular carcinoma cell line HepG2. J Biol Chem 276: 40968-40976, 2001.
30. Monto A and Wright TL: The epidemiology and prevention of hepatocellular carcinoma. Semin Oncol 28: 441-449, 2001.
31. Seeff LB: Natural history of chronic hepatitis C. Hepatology 36: S35-S46, 2002.
32. Romeo R and Colombo M: The natural history of hepatocellular carcinoma. Toxicology 181-182: 39-42, 2002.
33. Chen SH, Chen XH, Wang Y, Kosai K, Finegold MJ, Rich SS and Woo SL: Combination gene therapy for liver metastasis of colon carcinoma *in vivo*. Proc Natl Acad Sci USA 92: 2577-2581, 1995.
34. Chen SH, Kosai K, Xu B, Pham-Nguyen K, Contant C, Finegold MJ and Woo SL: Combination suicide and cytokine gene therapy for hepatic metastases of colon carcinoma: sustained antitumor immunity prolongs animal survival. Cancer Res 56: 3758-3762, 1996.
35. Caruso M, Pham-Nguyen K, Kwong YL, Xu B, Kosai KI, Finegold M, Woo SL and Chen SH: Adenovirus-mediated interleukin-12 gene therapy for metastatic colon carcinoma. Proc Natl Acad Sci USA 93: 11302-11306, 1996.
36. Terazaki Y, Yano S, Yuge K, Nagano S, Fukunaga M, Guo ZS, Komiya S, Shirouzu K and Kosai K: An optimal therapeutic expression level is crucial for suicide gene therapy for hepatic metastatic cancer in mice. Hepatology 37: 155-163, 2003.
37. Fukunaga M, Takamori S, Hayashi A, Shirouzu K and Kosai K: Adenoviral herpes simplex virus thymidine kinase gene therapy in an orthotopic lung cancer model. Ann Thorac Surg 73: 1740-1746, 2002.
38. Nagano S, Yuge K, Fukunaga M, Terazaki Y, Fujiwara H, Komiya S and Kosai K: Gene therapy eradicating distant disseminated micro-metastases by optimal cytokine expression in the primary lesion only: novel concepts for successful cytokine gene therapy. Int J Oncol 24: 549-558, 2004.
39. Matsumoto K, Kataoka H, Date K and Nakamura T: Cooperative interaction between alpha- and beta-chains of hepatocyte growth factor on c-Met receptor confers ligand-induced receptor tyrosine phosphorylation and multiple biological responses. J Biol Chem 273: 22913-22920, 1998.
40. Enari M, Sakahira H, Yokoyama H, Okawa K, Iwamatsu A and Nagata S: A caspase-activated DNase that degrades DNA during apoptosis, and its inhibitor ICAD. Nature 391: 43-50, 1998.
41. Sahara S, Aoto M, Eguchi Y, Imamoto N, Yoneda Y and Tsujimoto Y: Acinus is a caspase-3-activated protein required for apoptotic chromatin condensation. Nature 401: 168-173, 1999.
42. Llovet JM and Bruix J: Systematic review of randomized trials for unresectable hepatocellular carcinoma: chemoembolization improves survival. Hepatology 37: 429-442, 2003.
43. Schwartz JD and Beutler AS: Therapy for unresectable hepatocellular carcinoma: review of the randomized clinical trials-II: systemic and local non-embolization-based therapies in unresectable and advanced hepatocellular carcinoma. Anticancer Drugs 15: 439-452, 2004.
44. Shima N, Stolz DB, Miyazaki M, Gohda E, Higashio K and Michalopoulos GK: Possible involvement of p21/waf1 in the growth inhibition of HepG2 cells induced by hepatocyte growth factor. J Cell Physiol 177: 130-136, 1998.

45. Zhang H, Ozaki I, Mizuta T, Yoshimura T, Matsuhashi S, Hisatomi A, Tadano J, Sakai T and Yamamoto K: Mechanism of beta 1-integrin-mediated hepatoma cell growth involves p27 and S-phase kinase-associated protein 2. Hepatology 38: 305-313, 2003.
46. Wang X, De Frances MC, Dai Y, Pediaditakis P, Johnson C, Bell A, Michalopoulos GK and Zarnegar R: A mechanism of cell survival: sequestration of Fas by the HGF receptor Met. Mol Cell 9: 411-421, 2002.
47. Nagao M, Nakajima Y, Hisanaga M, Kayagaki N, Kanehiro H, Aomatsu Y, Ko S, Yagita H, Yamada T, Okumura K and Nakano H: The alteration of Fas receptor and ligand system in hepatocellular carcinomas: how do hepatoma cells escape from the host immune surveillance *in vivo*? Hepatology 30: 413-421, 1999.
48. Lee SH, Shin MS, Lee HS, Bae JH, Lee HK, Kim HS, Kim SY, Jang JJ, Joo M and Kang YK: Expression of Fas and Fas-related molecules in human hepatocellular carcinoma. Hum Pathol 32: 250-256, 2001.
49. Nishio K, Fujiwara Y, Miyahara Y, Takeda Y, Ohira T, Kubota N, Ohta S, Funayama Y, Ogasawara H, Ohata M, *et al*: Cis-diamminedichloroplatinum(II) inhibits p34cdc2 protein kinase in human lung-cancer cells. Int J Cancer 55: 616-622, 1993.
50. Muller M, Strand S, Hug H, Heinemann EM, Walczak H, Hofmann WJ, Stremmel W, Krammer PH and Galle PR: Drug-induced apoptosis in hepatoma cells is mediated by the CD95 (APO-1/Fas) receptor/ligand system and involves activation of wild-type p53. J Clin Invest 99: 403-413, 1997.
51. Muller M, Wilder S, Bannasch D, Israeli D, Lehlbach K, Li-Weber M, Friedman SL, Galle PR, Stremmel W, Oren M and Krammer PH: p53 activates the CD95 (APO-1/Fas) gene in response to DNA damage by anticancer drugs. J Exp Med 188: 2033-2045, 1998.
52. Wersto RP, Rosenthal ER, Seth PK, Eissa NT and Donahue RE: Recombinant, replication-defective adenovirus gene transfer vectors induce cell cycle dysregulation and inappropriate expression of cyclin proteins. J Virol 72: 9491-9502, 1998.
53. Kuhn H, Liebers U, Gessner C, Karawajew L, Ruppert V, Schumacher A, Witt C and Wolff G: Infection of cells with replication deficient adenovirus induces cell cycle alterations and leads to downregulation of E2F-1. Biochim Biophys Acta (BBA) - Mol Cell Res 1542: 106-115, 2002.

Diffuse encephaloventriculitis and substantial leukoencephalopathy after intraventricular administration of recombinant adenovirus

Tsuyoshi Tada*, John Bang Nguyen†, Yasuyuki Hitoshi†, Nathan P. Watson†, Jeffrey F. Dunn‡, Shinji Ohara§, Satoshi Nagano¶, Ken-ichiro Kosai¶ and Mark A. Israel†

*Department of Neurosurgery Shinshu University School of Medicine, Asahi 3-1-1, Matsumoto 390-8621, Japan
†Israel Laboratory, NCCC Research, Norris Cotton Cancer Center, Dartmouth Medical School, Hanover NH 03755, USA
‡Biomedical NMR Laboratory, Department of Diagnostic Radiology, Dartmouth Medical School, HB 7786, Hanover NH 03755, USA
§Department of Neurology, National Chushin Matsumoto Hospital, Kotobuki 811, Matsumoto 390-0021, Japan
¶Division of Gene Therapy and Regenerative Medicine, Cognitive and Molecular Research Institute of Brain Diseases, Kurume University, Asahi-machi 67, Kurume 830-0011, Japan

Objectives: *The use of recombinant adenovirus as a vehicle for gene transfer into ependymal cells is a potential therapeutic tool for the treatment of various neural disorders. However, gene transfer into the ependymal cells of the ventricular wall is associated with high-level expression of the transferred gene, which declines rapidly. The purpose of this study is to understand the cause of this early decline in gene expression.*

Methods: *Different doses of adenovirus-expressing β-galactosidase (Ad-β-gal) were injected into the lateral brain ventricle of C57BL/6 mice, and the brains were observed histologically and with magnetic resonance (MR) imaging for a month.*

Results: *Inoculation of the lateral ventricle with more than 1×10^8 viral particles (2.6×10^6 pfu) resulted in a rapid decline of β-gal expression. MR imaging indicated gradual ventriculomegaly and histological analysis showed the loss of the ependymal cells from the ventricular wall, lymphocytes infiltration near the wall, degeneration of myelinated fibers and apoptosis in the external capsule. Reactive astrocytes proliferated in the external capsule 17 days following inoculation. To avoid this irreversible brain atrophy, the inoculated adenovirus should be reduced to less than 1×10^7 particles (2.6×10^5 pfu) in mice.*

Discussion: *Our results indicate the presence of a unique and diffuse immune response of the brain; therefore, the clinical use of recombinant virus for intraventricular gene transfer must be carefully evaluated.* [Neurol Res 2005; **27**: 378–386]

Keywords: Adenovirus; encephaloventriculitis; leukoencephalopathy; mouse; ventricles

INTRODUCTION

Because systematically administrated bioactive substances cannot efficiently pass the blood–brain barrier[1], therapeutic proteins and peptides must be delivered directly in the central nervous system (CNS) for the treatment of neural disorders such as subarachnoid dissemination of malignant tumors and ischemic disorders[2–4].

The ependymal cell is an ideal target for gene therapy because gene products released into the cerebrospinal fluid (CSF) may access various cells in the CNS through the Virchow–Robbins spaces[5–7].

Recombinant adenovirus provides a suitable vehicle for gene transfer into cells of the CNS, because of its ability to efficiently deliver genes into non-replicating cells[8,9]. Almost all trans-gene experiments targeting ependymal cells have used recombinant adenovirus as vehicles for gene transfer[10–20]. However, despite favorable results in animal models, the efficacy of intraventricular administration of recombinant virus has not yet been proven in human studies[21,22]. Viral inoculation immediately stimulates both the humoral and cellular immune response of the host. This immune response has been shown to be a determining factor for the duration of the gene expression[23,24]. In the liver, expression of transferred genes declines rapidly; however, gene transfer into the brain has been reported to result in long-term expression[8,25,26]. Therefore, the brain has often been regarded as an organ that is protected from immune reactions. To realize the clinical

Correspondence and reprint requests to: [tadatsu@hsp.md.shinshu-u.ac.jp] Accepted for publication December 2004.

10.1179/016164105X22075

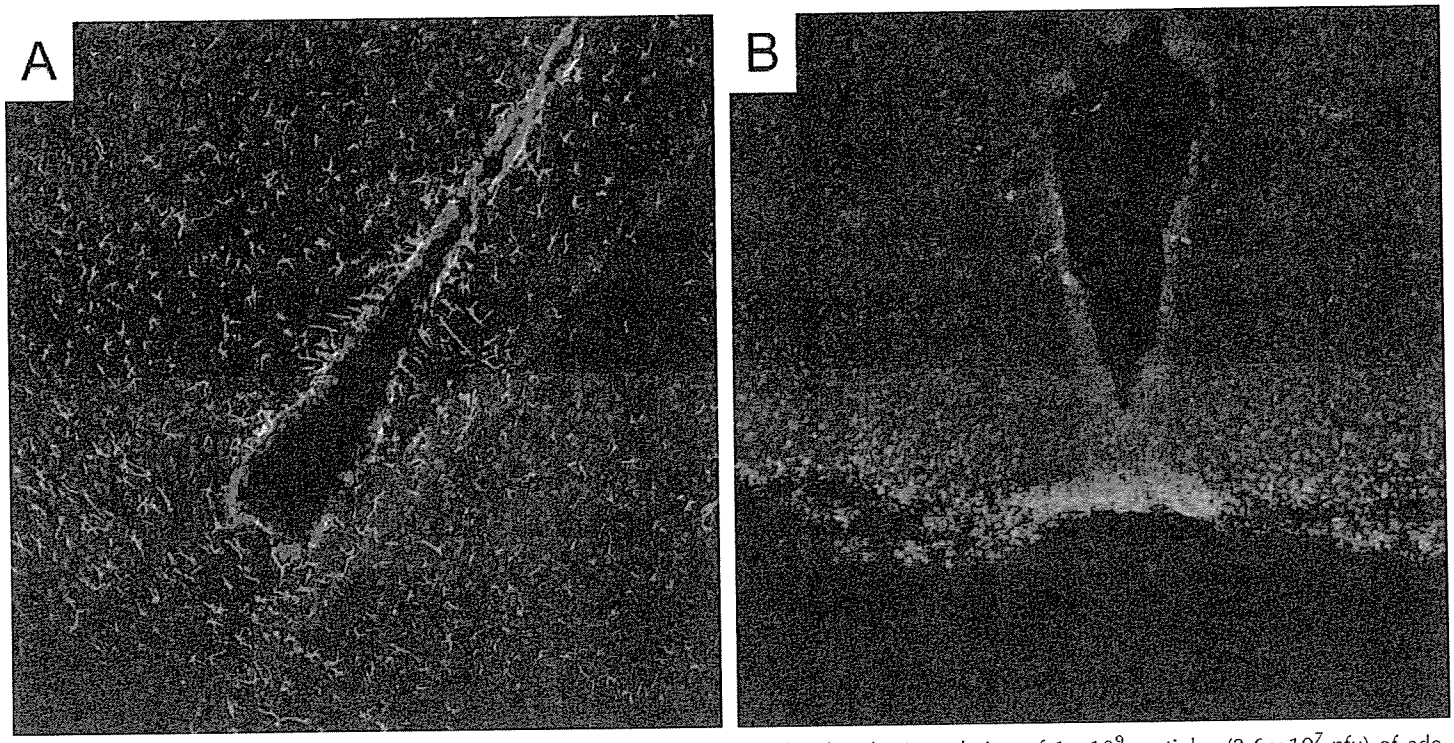

Figure 1: Expression of β-gal in the ependymal layer lining the third ventricle after the inoculation of 1×10^9 particles (2.6×10^7 pfu) of adenovirus. (A) The brain 4 days after inoculation. The section was incubated with rabbit anti-β-gal antibody, and goat anti-GFAP antibody. The secondary antibodies used were FITC-conjugated anti-rabbit antibody and RR-conjugated anti-goat antibody. RR-positive cells indicate ependymal cells. (B) The brain 7 days after the inoculation. The section was treated with rabbit anti-β-gal antibody and FITC-conjugated anti-rabbit antibody. Only a few β-gal-positive cells remain in the third ventricular wall

application of intraventricular gene therapy, we should more carefully examine the inflammatory and immune response of the host after the virus inoculation in the CNS[27,28].

In this study, we examined the cause of the early decline of gene expression from the ventricular wall. Magnetic resonance (MR) imaging and histological observations indicated an immune response following viral inoculation of both the brain parenchyma and the ventricular wall. However, the immune response in the ventricle was much more severe and was associated with diffuse encephalo-ventriculitis and substantial brain atrophy.

MATERIALS AND METHODS

Animals and reagents

C57BL/6 mice were purchased from Charles River Laboratories (Wilmington, MA). These mice were housed in a polycarbonate cage in the Animal Care Facility at the Dartmouth School of Medicine, and were fed with a commercial diet (LM-485 Mouse/Rat sterilizable diet 7012, Madison, WI). All mice were kept under a 12:12 hour dark–light cycle (lights turned on at 09:00). The room was kept at 24 ± 2°C and at 55 ± 10% relative humidity. Animal care was conducted in accordance with the 'Principles of Laboratory Animal Care' formulated by the National Society for Medical Research[29] and the 'Guide for the Care and Use of Laboratory Animals' prepared by the National Academy of Sciences and published by the National Institutes of Health (NIH Publication No. 86-23, revised 1996)[30].

Recombinant adenoviral vectors

E1 and E3 deleted adenoviral vector encoding β-galactosidase (Ad-β-gal) was prepared as described by Mizuguchi and Kay[32].

Anesthesia

Mice were sedated by intraperitoneal injection of a mixture of ketamine hydrochloride (2.5 mg/mouse) and medetomidine (0.025 mg/mouse). To reverse the anesthesia, antipamezole hydrochloride (0.125 mg/mouse) was injected[33].

Stereotaxic surgery

Once sedated, mice were placed in a stereotaxic frame (Model 900, Pembroke Pines, FL). A hole was made in the skull, 0.6 mm caudal from the coronal suture and 1 mm lateral from the midline. Ad-β-gal (1×10^9, 1×10^8, 1×10^7 particles/10 μl/mouse) was injected at a depth of 4 mm with a 10 μl Hamilton syringe on day 0.

MR imaging

Mouse brains were examined on days 3, 8, 17 and 29 with 7.0-tesla whole-body MR imaging. Others were killed after MR imaging. T2-weighted images were obtained with sequences (coronal plane; slice, 0.5 cm; TE, 90 milliseconds; TR, 2000 milliseconds).

Histological procedures

Deeply sedated mice were perfused with cold 4% paraformaldehyde (Electron Microscopy Sciences,

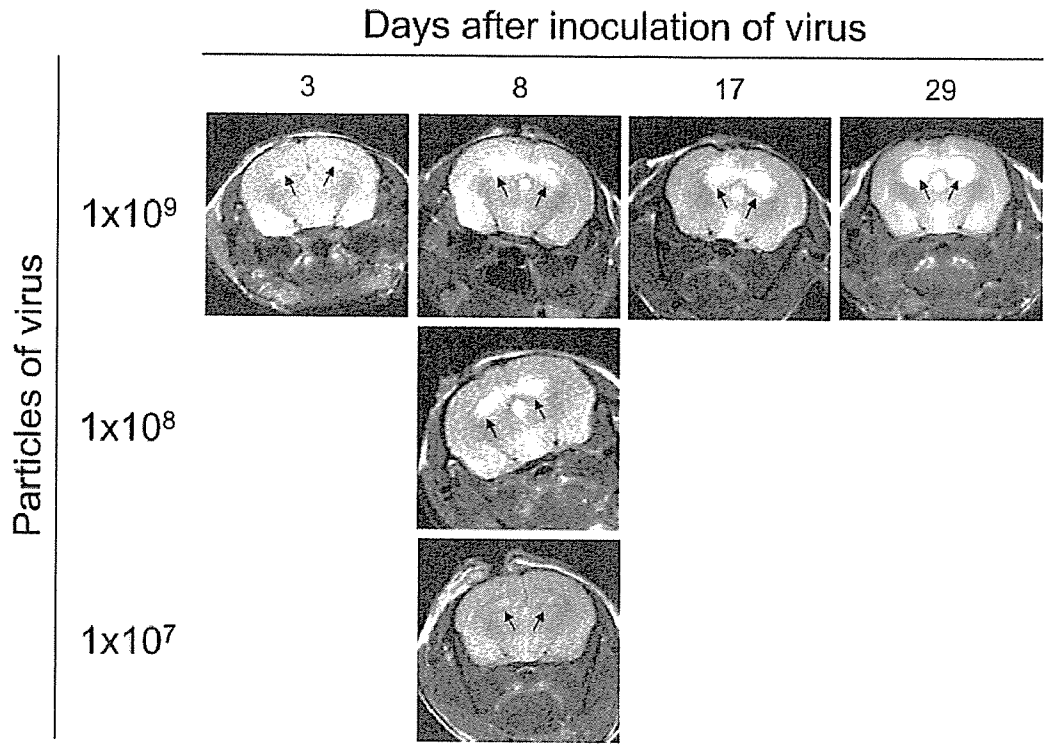

Figure 2: MR images taken at days 3, 8, 17 and 29 following the inoculation of 1×10^9 particles (2.6×10^7 pfu) of adenovirus encoding β-gal, and 8 days after the inoculation of 1×10^8 or 1×10^7 viral particles. The images taken 3 days after the inoculation of 1×10^9 particles as well as 8 days after the inoculation of 1×10^7 particles of the virus were consistent with a normal brain. The images taken 8 days after the inoculation of 1×10^9 and 1×10^8 viral particles showed mild ventriculomegaly. The ventricular system gradually dilated between days 17 and 29. Arrows indicate lateral ventricles

Hatfield, PA) in 0.1% phosphate-buffered saline, pH 7.4. One-half of the brain was dehydrated with a gradient sucrose solution, and was frozen at −80°C. The other half was embedded in paraffin.

The frozen brain was cut in 20 μm sections, and the sections were incubated with rabbit polyclonal anti-β-gal antibody (1:5000), IgG fraction (Cortex Biochem, San Leandro, CA) or goat polyclonal anti-glial fibrillary acidic protein (GFAP) antibody (1:5000). Fluorescein isothiocyanate (FITC)-conjugated horse anti-rabbit antibody or rhodamin red (RR)-conjugated horse anti-goat antibody (Jackson Immuno Research Laboratories, West Grove, PA) were used as secondary antibodies. Specimens were mounted in VECTASHIELD mounting medium with DAPI (Vector, Burlingame, CA).

Paraffin-embedded brains were cut in to 4 μm sections and stained with HE. Immunohistochemical studies were performed on the paraffin-embedded sections using the avidin–biotin–peroxidase complex (ABC) method with a Vectastain ABC kit (Vector, Burlingame, CA). The primary antibodies specific for apoptotic cells, myelin basic protein (MBP) and GFAP were polyclonal rabbit anti-single stranded DNA antibody (1:100) (DakoCytomation Co. Ltd, Kyoto, Japan), polyclonal rabbit anti-human MBP (1:1) (DakoCytomation), rabbit anti-Cow GFAP (1:500) (DakoCytomation), respectively.

RESULTS

Gene transfer to ependymal cells

Four days after the inoculation of 1×10^9 viral particles (2.6×10^7 pfu) in the lateral ventricle wall, double-staining with anti-GFAP and anti-β-gal antibodies shows the presence of a single layer of β-gal-positive cells in the third ventricular wall (*Figure 1A*). These β-gal-positive cells did not co-stain with the GFAP antibody. Seven days after the inoculation of 1×10^9 particles (2.6×10^7 pfu), staining with an FITC-conjugated anti-β-gal antibody shows a reduction in the number of β-gal-positive cells, and only a few positive cells were observed in the third ventricular wall and the parenchyma (*Figure 1B*).

MR follow-up after intraventricular inoculation of virus

MR imaging of the brains at day 3 following intraventricular inoculation of 1×10^9 particles (2.6×10^7 pfu) showed no brain abnormalities (*Figure 2*). Similarly, MR images taken at day 8 following inoculation of 1×10^7 particles (1×10^5 pfu) were consistent with a normal brain. In contrast, the MR images taken 8 days after the inoculation of 1×10^9 and 1×10^8 particles showed mild ventriculomegaly, and the ventricular system appeared more dilated at days 17 and 29.

HE staining of the brain after intraventricular inoculation of the virus

Intraventricular inoculation of more than 1×10^8 viral particles resulted in the infiltration of mononuclear cells into the ventricular wall and perivascular space, and the concomitant loss of ependymal cells from the ventricular wall (*Figure 3*).

Figure 4 shows HE staining of the external capsule at days 8, 17 and 29 days following inoculation of 1×10^9

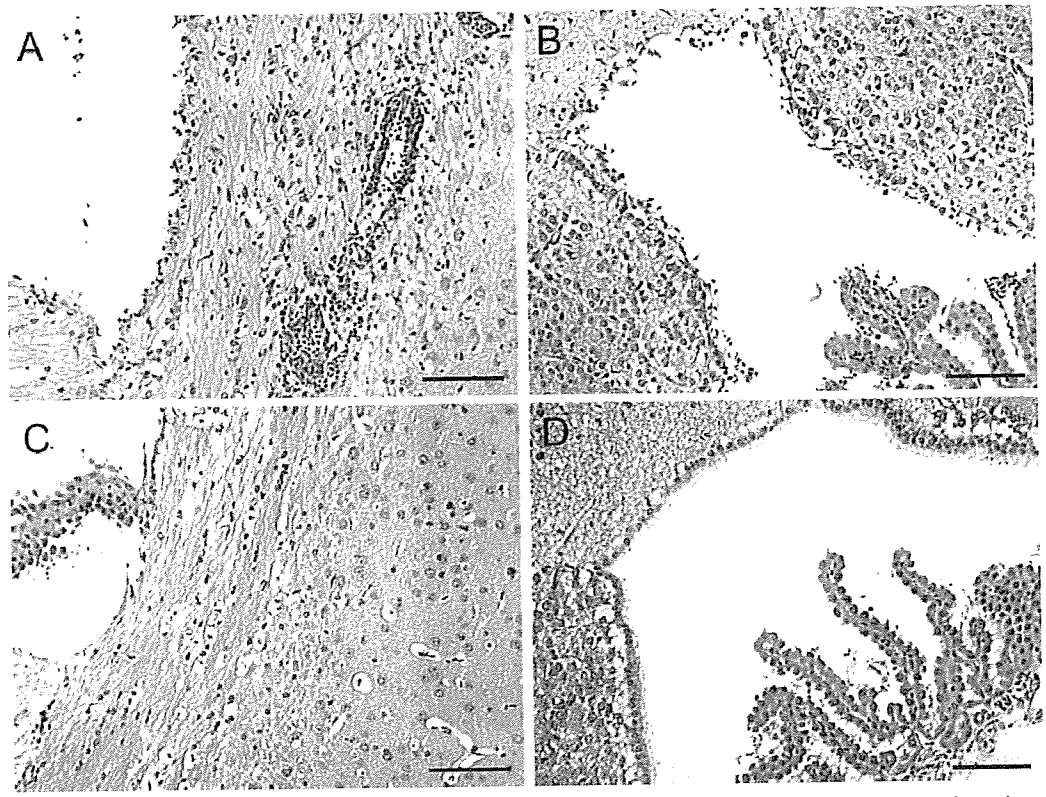

Figure 3: HE staining of the paraventricular portion of the lateral ventricle and the third ventricle 8 days following inoculation of 1×10^8 particles (2.6×10^6 pfu) (A and B) or 1×10^7 particles (2.6×10^5 pfu) (C and D) of adenovirus encoding β-gal, respectively. The infiltration of mononuclear cells into the ventricular wall and perivascular space, and loss of ependymal cells from the ventricular wall was apparent after the inoculation of 1×10^9 viral particles. Bar=100 μm

particles (2.6×10^7 pfu) and 1×10^7 particles (2.6×10^5 pfu), respectively. An edematous change is clearly apparent in the external capsule following inoculation with the higher dose of 1×10^9 particles (2.6×10^7 pfu).

Analysis at a higher resolution reveals a microcystic change in the tissue surrounding the external capsule following the inoculation of 1×10^9 viral particles. In addition, proliferation of cells with large, clear nuclei was observed in the external capsule at days 17 and 29. These phenomena were not observed following the intraventricular inoculation with the lower dose of 1×10^7 particles (*Figure 5*).

Immunostaining of the brain after intraventricular administration of the virus

To estimate the proliferation of cells having large clear cells in the external capsule in HE staining, we examined them immunohistologically. Immunostaining for MBP showed a decrease in myelinated fibers as well as fragmentation of these fibers in the external capsule following the inoculation of 1×10^8 viral particles. A decrease and fragmentation of myelinated fibers did not occur following inoculation with the lower dose of 1×10^8 viral particles (*Figure 6*).

Inoculation of 1×10^9 particles resulted in significant apoptosis in the bilateral external capsule by day 8 (*Figure 7*), but only a few apoptotic cells were observed at days 17 and 29. Inoculation of 1×10^7 particles did not result in apoptosis by day 8 (data not shown).

The cytoplasm of the cells having a large clear nucleus proliferated in the external capsule at 17 and 29 days following inoculation of the virus was positive for anti-GFAP antibody (*Figure 8*)

DISCUSSION

When recombinant adenovirus is inoculated into the brain parenchyma, $CD4^+$ and $CD8^+$ T cells, and macrophages soon accumulate and MHC I is up-regulated in the vascular endothelium within 24 hours[24,34]. Because the immune response is also elicited by adenovirus that does not express β-gal, as well as ultraviolet-irradiated virus, the virus particles by themselves can induce inflammation at the injection site (our personal data)[34]. Despite the immune response, the expression of the transferred gene is apparent by the next day and numerous positive cells are seen after 60 days in the rat brain parenchyma[34]. Interestingly, the duration of gene expression is substantially longer in the brain than in other organs[25]. For example, Davidson *et al.* inoculated 5×10^7 pfu of Ad-β-gal into the mouse caudate putamen, and the gene expression continued for at least 8 weeks[26]. This long-term expression is generally explained by the observation that immune responses are typically less strong in the brain when compared with other organs[35]. Lowenstein described that up to 1×10^8 pfu of adenoviral vectors

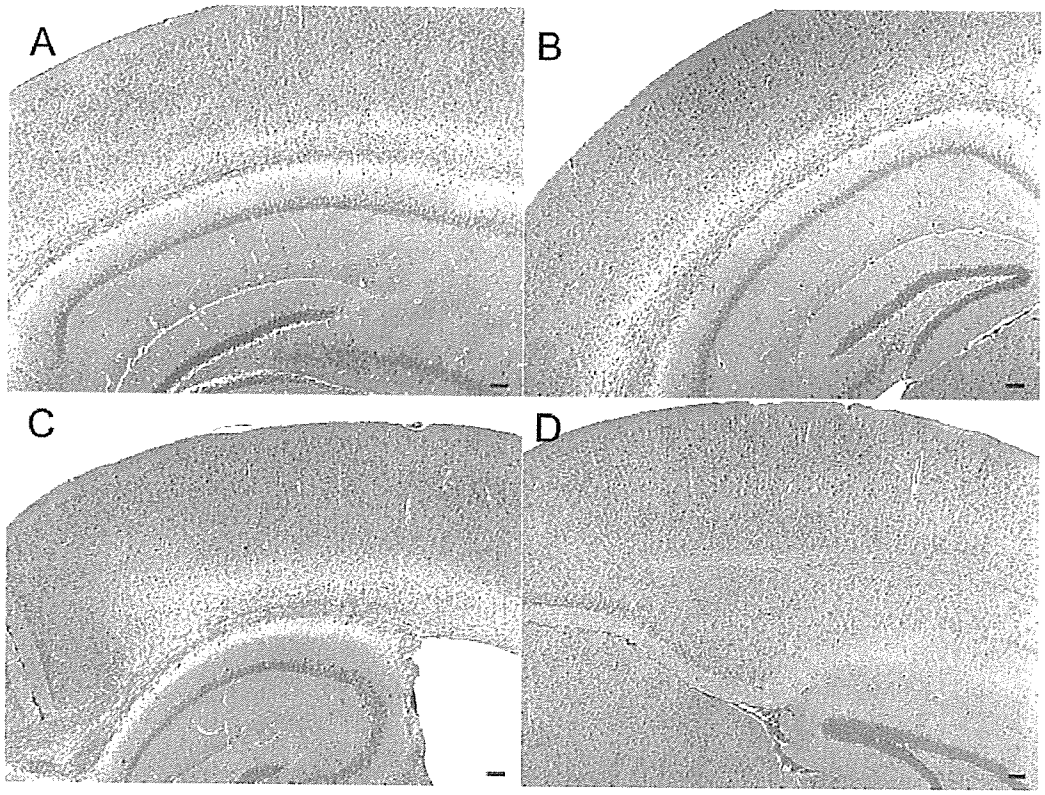

Figure 4: HE staining of the external capsule of the brains at days 8 (A), 17 (B) and 29 (C) following inoculation of 1×10^9 particles (2.6×10^7 pfu), or 1×10^7 of adenovirus encoding β-gal (2.6×10^5 pfu) (D). The edematous change was apparent near the external capsule of the brains at days 8, 17 and 29 following inoculation of 1×10^9 viral particles. Bar=100 μm

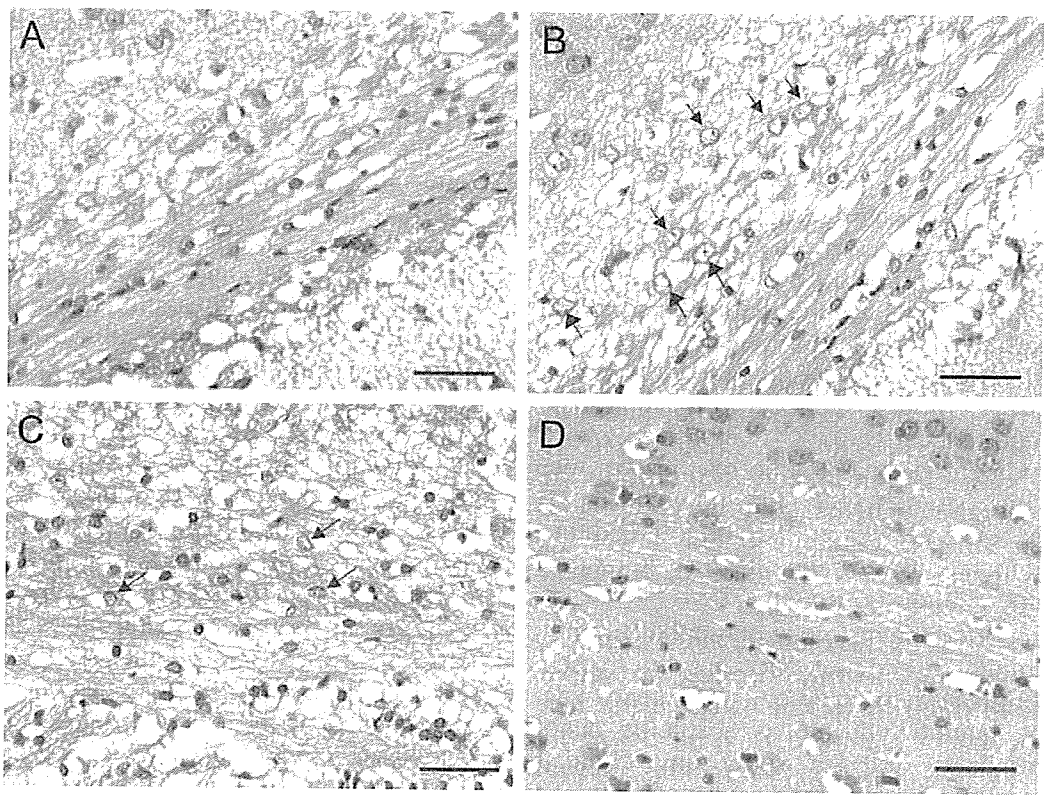

Figure 5: HE staining of the external capsule of the brain at days 8 (A), 17 (B) and 29 (C) following inoculation of 1×10^9 particles (2.6×10^7 pfu), or 1×10^7 of adenovirus encoding β-gal (2.6×10^5 pfu) (D). Microcystic change is apparent in the tissue surrounding the external capsule of the brains at days 8, 17 and 29 following inoculation of 1×10^9 viral particles. Many cells characterized by large clear nuclei proliferated into the external capsule of the brains 17 and 29 days after the inoculation of 1×10^9 viral particles (arrow). Bar=50 μm

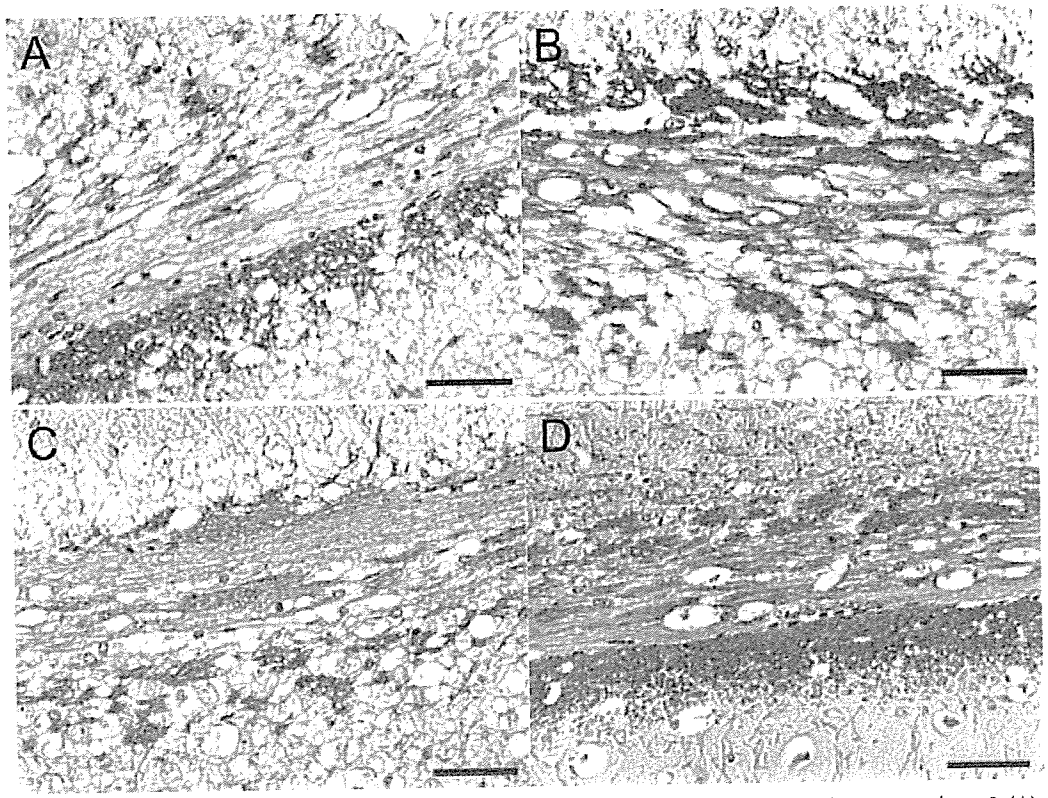

Figure 6: Immunostaining for myelinated fibers of the external capsule of the brains at days 8 (A), 17 (B) and 29 (C) following inoculation of 1×10^9 particles (2.6×10^7 pfu) of adenovirus encoding β-gal, or 8 days after the inoculation of 1×10^8 viral particles (D). The number of myelinated fibers decreased and the remaining fibers appeared fragmented at days 8 (A), 17 (B) and 29 (C) following inoculation of 1×10^9 viral particles (2.6×10^7 pfu). Bar=50 μm

injected into a single mouse brain site resulted in acute, dose-dependent, inflammation, which was reversible within 30 days, and was accompanied with very limited cytotoxicity. However, injection of 1×10^9 pfu resulted in massive cytotoxicity and chronic unremitting inflammation[36].

In contrast to intraparenchymal inoculation, histological studies on the gene transfer into ependymal cells have been limited (*Table 1*). Most of these studies used a recombinant adenovirus as the vehicle for gene transfer. Viral particle doses varied between 1.2×10^6 and 1×10^{10} pfu. The peak time of gene expression varied between days 1 and 9, except for the studies by Davidson *et al.* and Ghodsi *et al.*[16,37]. Ghodsi *et al.* did not mention the difference in immune response in the brain between intraparenchymal and intraventricular inoculation of the virus. Davidson *et al.* only traced the expression of the marker gene in the olfactory bulb after intraventricular inoculation of the virus.

Driesse *et al.* reported the histology of monkey brains, in which recombinant adenovirus encoding the herpes simplex virus-conjugated thymidine kinase gene was injected into the lateral ventricle as a suicide gene therapy. The monkeys did not show any clinical symptoms, but $CD4^+$ T cells, $CD8^+$ T cells and B ($CD19^+$) lymphocytes, plasma cells and histiocytic cells infiltrated the choroid plexus and the superficial layer of the parenchyma resulting in the loss of some ependymal cells at day 21[38]. It was suggested that the intraventricular administration of recombinant virus caused a strong immune response. Because their observations were limited to days 3 and 21 post-administration, they did not observe the expected subsequent brain atrophy.

Here, we show the successful transfer of the β-gal gene into the ependymal layer by the intraventricular inoculation of 1×10^9 particles (2.6×10^7 pfu) of adenovirus. However, β-gal expression rapidly declines and β-gal-positive cells have almost completely disappeared by day 7. Histological examination indicates ventricular dilatation accompanied by diffuse periventricular lymphocytic infiltration, and loss of ependymal cells from the ventricular wall of the brain. The rapid decline of β-gal expression can be easily explained by this loss of ependymal cells. Follow-up MR images showed progressive ventriculomegaly and further histologic analysis revealed edematous changes in the center of the hemisphere, most prominent in the external capsule.

Apoptotic cells were often found in the external capsule of the brain 8 days following inoculation with the high dose of 1×10^9 viral particles. These apoptotic cells are likely to be oligodendrocytes because of their linear arrangement in the external capsule and because their cytoplasm was not positive for GFAP. Immunostaining for MBP showed a clear decrease and fragmentation of myelinated fibers of the external capsule of the brain inoculated with 1×10^9 particles, which was associated with proliferation of astrocytes in the external capsule.

Astrocytes produce various cytokines such as tumor necrosis factor following viral infection[39]. In contrast,

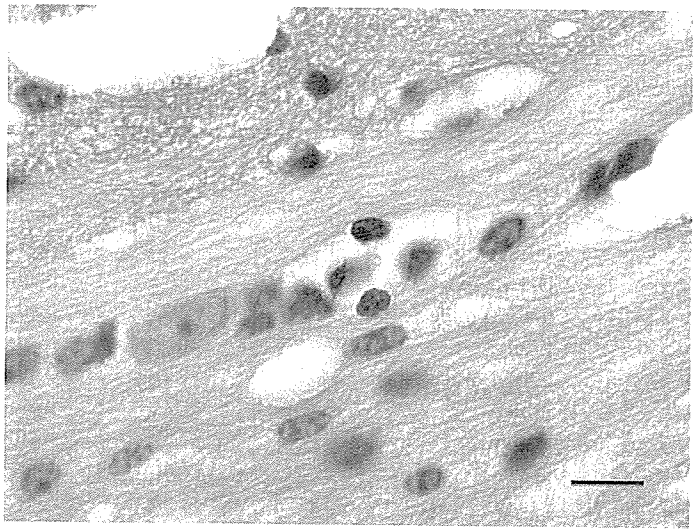

Figure 7: Immunostaining for single-stranded DNA 8 days following inoculation of 1×10^9 particles (2.6×10^7 pfu) of adenovirus encoding β-gal, showing two immunoreactive nuclei in the external capsule of the cerebrum. Bar=10 μm

neurons and oligodendrocytes are sensitive to the effects of the inflammatory cytokines and reactive oxygen species, which are released during an inflammatory response, and Wallerian degeneration is regulated by some inflammatory cytokines[40,41]. These inflammatory cytokines also stimulate the proliferation of reactive astrocytes[42]. Our observations are consistent with these reports.

Thus, the immune response following intraventricular administration of recombinant adenovirus appears to be different from the immune response to intraparenchymal administration of the virus. Normal brain has dendritic cells in the choroid plexus and meninges[43]. The antigen presenting cells in the CSF space would play an important role in inducing the stronger immune response of the CNS, when the virus is injected into the CSF space. Further research is required to elucidate the underlying mechanism of the differences in immune response between the CSF and parenchyma.

Care must be taken when considering that the observed ventriculomegaly depended upon brain

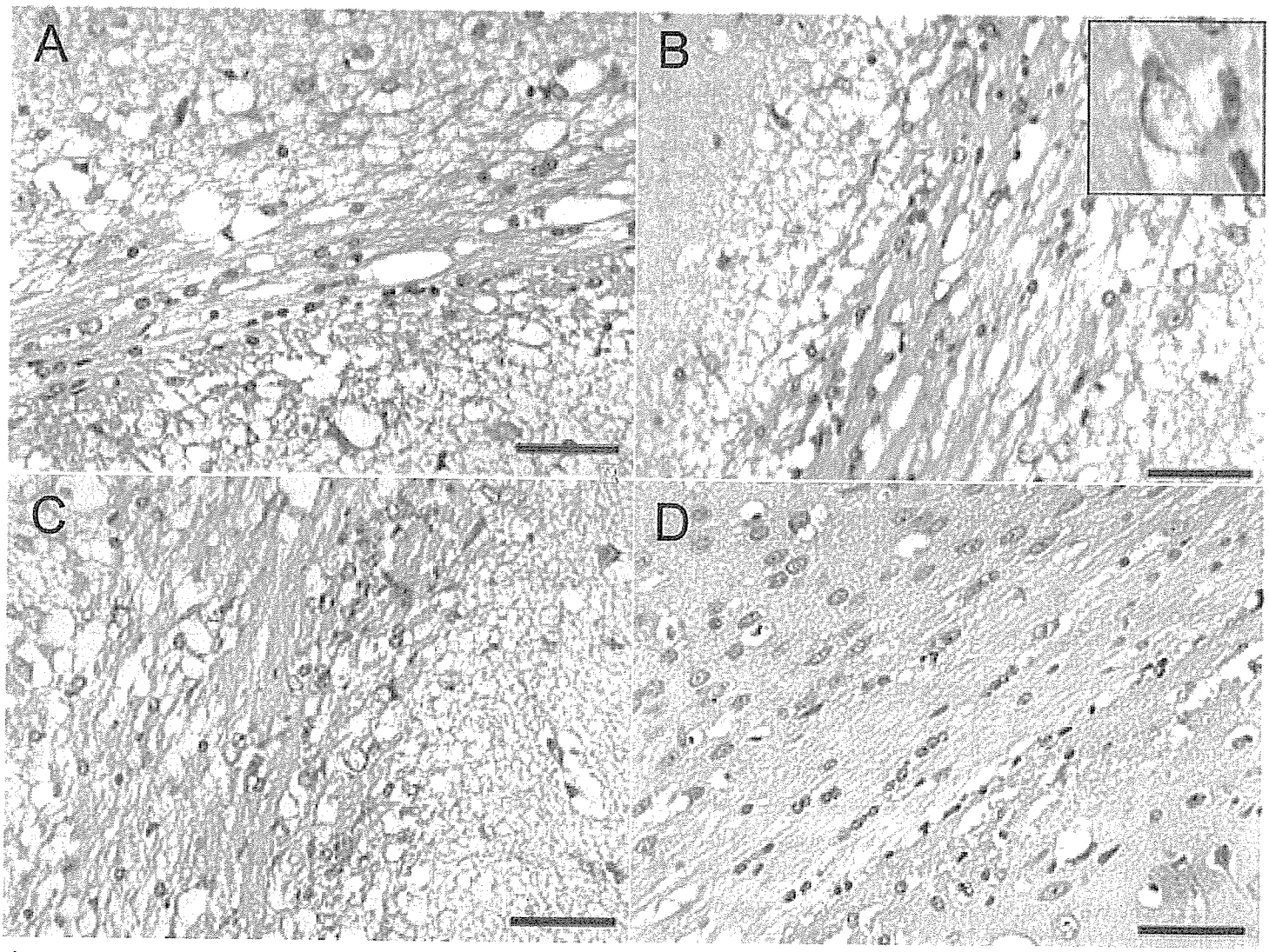

Figure 8: Immunostaining for GFAP of the external capsule of the brains at days 8 (A), 17 (B) and 29 (C) following inoculation of 1×10^9 particles (2.6×10^7 pfu) of adenovirus encoding β-gal and 8 days after the inoculation of 1×10^8 viral particles (2.6×10^6 pfu) (D). Only a few GFAP-positive cells were observed in the external capsule 8 days after the inoculation of 1×10^9 and 1×10^7 viral particles. However, the cytoplasm of the cells with large clear nuclei that proliferated in the external capsule 17 and 29 days after the inoculation were found to be GFAP-positive. Bar=50 μm. The magnified corner in (B) indicates the GFAP-positive cell with a large nucleus